

Introduction to cosmology and dark matter

A. De Simone

SISSA and INFN Sezione di Trieste, Trieste, Italy

Abstract

These are the lectures notes for the course on Introduction to Cosmology and Dark Matter given at the CERN European School for High Energy Physics (ESHEP) 2018. The audience consists of graduate students with particle physics background.

Keywords

Cosmology; universe dynamics; expansion; dark matter; lectures.

1 Introduction

1.1 Motivations and Outline

These lectures are addressed to an audience of graduate students in experimental particle physics. So the first question usually is:

“Why should a particle physicist care about Cosmology”?

There are at least three main reasons to attend an introductory course on cosmology such as this one.

1. Cosmology provides insights on particle physics at energy scales which are impossible to probe on Earth. In the very early moments after the Big Bang the universe had a temperature (or energy) which would never be reachable again. So the by-products of the early universe dynamics we can measure today give us information about the physics at incredibly high energies.
2. Cosmology provides alternative (sometimes competitive) constraints on particle physics properties (e.g. neutrino physics, dark matter, etc.)
3. Cosmology provides motivations for (or completions of) particle physics models beyond the Standard Model. The need to solve cosmological issues like inflation, baryogenesis, dark matter calls for new particle physics which is able to model them and make predictions.

In these lectures I will give an overview of the Standard Model of Cosmology, its main successes and its drawbacks, with particular focus on the particle physics side.

In Lecture 1, I will describe the universe around us, its dynamics, the energy budget (Section 2), and provide introductory information about the 3 pillars constituting the Standard Model of Cosmology: Expansion, Big Bang Nucleosynthesis, Cosmic Microwave Background (Sections 2, 3, 4).

In Lecture 2, I will discuss the problem of Dark Matter (Section 5).

In Lecture 3, the main pitfalls of Standard Big Bang Cosmology and their possible resolution with the inflationary paradigm are described in Section 6, and then I conclude the course by mentioning the problem of the Baryon Asymmetry of the universe and some models of Baryogenesis in Section 7.

1.2 Warm-up

Throughout the course we will adopt the so-called “natural units”, where the dimensions of basic physical quantities are related as

$$[\text{Energy}] = [\text{Mass}] = [\text{Temperature}] = [\text{Length}]^{-1} = [\text{Time}]^{-1}, \quad (1)$$

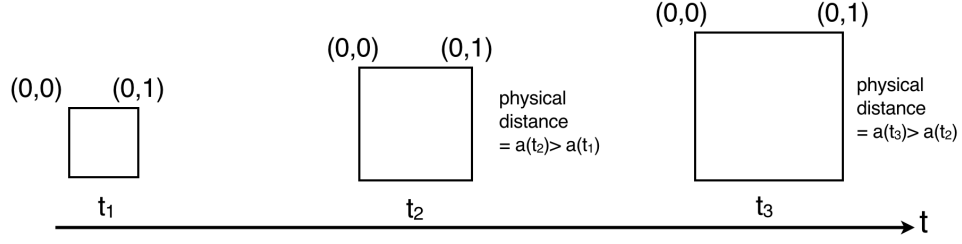


Fig. 1: Expansion of physical distances.

and the main physical constants are set as

$$\hbar = c = k_B = 1, \quad (2)$$

from which it follows that

$$1 = \hbar \cdot c \simeq 197.33 \text{ MeV} \cdot \text{fm} = 1.9733 \times 10^{-14} \text{ GeV} \cdot \text{cm}, \quad (3)$$

so

$$1 \text{ GeV}^{-1} = 1.9733 \times 10^{-14} \text{ cm} = 1.9733 \times 10^{-14} \frac{\text{cm}}{c} = 6.5822 \times 10^{-25} \text{ s} \quad (4)$$

The fundamental mass scale of gravitational interactions is the Planck mass $M_P = 1.22 \times 10^{19} \text{ GeV}$, while astronomical distances often appear in units of $1 \text{ pc} = 3.08 \times 10^{18} \text{ cm}$.

2 The universe around us

2.1 Kinematics of the universe

2.1.1 Expansion

From observations of the universe around us we can draw the conclusion that the universe is expanding. If you look at any two points in space, their relative distance was smaller in the past. In fact, the observation of red-shifted spectra of distant galaxies firmly supports the idea that the universe is expanding.

In an expanding universe, the physical distances between two points get larger and larger. They are proportional to a factor measuring the expansion of the universe: the *scale factor* $a(t)$ (Fig. 1). The velocity v at which a galaxy at distance d is going away from us is governed by the Hubble law

$$v = H_0 d, \quad (5)$$

where the velocity v is related to the wavelengths of the photon emitted and observed

$$v = \frac{\lambda_{\text{observation}} - \lambda_{\text{emission}}}{\lambda_{\text{emission}}} \equiv z, \quad (6)$$

with z being the *redshift* of the emission time t_e with respect to the present time t_0

$$1 + z \equiv \frac{\lambda_{\text{observation}}}{\lambda_{\text{emission}}} = \frac{a(t_0)}{a(t_e)}, \quad (7)$$

measuring how much the universe has expanded since the emission of that photon. By Taylor-expanding the ratio of scale factors around the present time t_0

$$\frac{a(t)}{a(t_0)} = 1 + H_0(t - t_0) - \frac{1}{2}q_0 H_0^2(t - t_0)^2 + \dots \quad (8)$$

where the local expansion rate today (‘Hubble constant’) is

$$H_0 \equiv \left. \frac{\dot{a}}{a} \right|_{t_0}. \quad (9)$$

The linear term in Eq. (8) gives the Hubble law Eq. (5), while the quadratic term depends on the deceleration parameter q

$$q_0 \equiv - \left. \frac{\ddot{a}}{aH_0^2} \right|_{t_0} = - \left. \frac{\ddot{a}a}{\dot{a}^2} \right|_{t_0}, \quad (10)$$

and it encodes the deviations from the Hubble law. The latest measurement [1] give

$$1/H_0 \simeq 1.4 \times 10^{10} \text{ yrs} \simeq 4.3 \text{ Gpc} \simeq 1.3 \times 10^{26} \text{ m}, \quad (11)$$

for the ‘Hubble time’, or ‘Hubble length’, and it is customary to define

$$h \equiv \frac{H_0}{100 \text{ km s}^{-1} \text{ Mpc}^{-1}} \simeq 0.67. \quad (12)$$

When observed on very large scales ($> 100 \text{ Mpc}$), the universe around us appears to be

- **homogenous**: the distribution of matter in the universe has a roughly constant density, or in other words the 2-point function of galaxies and galaxy clusters is much smaller than the Hubble length $1/H_0$;
- **isotropic**: if the expansion of the universe were not isotropic, we would observe large temperature anisotropies in the Cosmic Microwave Background.

The invariance under rotations is around any point of the Universe, so it is isotropic.

These observations lead us to consider that no observer is special and there are no preferred directions, so the universe is homogenous and isotropic (Cosmological Principle).

2.1.2 Friedmann-Robertson-Walker metric

We now want to build a metric describing a homogeneous and isotropic universe. The Friedmann-Robertson Walker metric is

$$ds^2 = dt^2 - a(t)^2 \left[\frac{dr^2}{1 - kr^2} + r^2(d\theta^2 + \sin^2\theta d\phi^2) \right], \quad (13)$$

where the parameter k can take three values

$$k = \begin{cases} +1 & \text{positive spatial curvature} \\ 0 & \text{zero spatial curvature} \\ -1 & \text{negative spatial curvature} \end{cases} \quad (14)$$

The scalar curvature of 3-dimensional spatial slices is

$$|{}^3\mathcal{R}| = \frac{6|k|}{a^2} \equiv \frac{6}{R_{\text{curv}}^2}, \quad (15)$$

where R_{curv} is a sort of curvature radius of the universe.

2.2 Dynamics of the universe

2.2.1 Einstein equations

The laws of gravity are the Einstein Equations, where the spacetime metric $g_{\mu\nu}$ and its corresponding Ricci tensor $R_{\mu\nu}$ and Ricci scalar R are related to energy content expressed through the energy-momentum tensor $T_{\mu\nu}$

$$R_{\mu\nu} - \frac{1}{2}g_{\mu\nu}R = 8\pi G_N T_{\mu\nu} + \Lambda g_{\mu\nu}, \quad (16)$$

where G_N is the Newton constant and we also included the cosmological constant term Λ .

The energy-momentum tensor for a perfect fluid with pressure p , energy density ρ and 4-velocity u^μ is

$$T_{\mu\nu} = (p + \rho)u_\mu u_\nu - pg_{\mu\nu}, \quad (17)$$

which assumes a diagonal form in the reference frame of the fluid (comoving frame) where $u^\mu = (1, 0, 0, 0)$

$$T_{\mu\nu} = \begin{pmatrix} \rho & 0 & 0 & 0 \\ 0 & -p & 0 & 0 \\ 0 & 0 & -p & 0 \\ 0 & 0 & 0 & -p \end{pmatrix}. \quad (18)$$

The energy-momentum conservation law is simply expressed as the vanishing of the covariant derivative of the energy-momentum tensor:

$$\nabla_\mu T^{\mu\nu} = 0, \quad (19)$$

whose $\nu = 0$ component in an expanding universe reads

$$\dot{\rho} + 3\frac{\dot{a}}{a}(\rho + p) = 0, \quad (20)$$

which is also known as ‘‘continuity equation’’. Alternatively, from the first law of thermodynamics $dU + pdV = TdS$, together with entropy conservation $dS = 0$, one gets

$$dU + pdV = 0 \implies d(a^3\rho) + pd(a^3) = 0, \quad (21)$$

which is the same as Eq. (20).

2.2.2 Fluids

The perfect fluids are characterized by a proportionality relation between energy density and pressure

$$p = w\rho \quad (22)$$

where w is constant in time. In this case, the continuity equation in Eq. (20) becomes

$$\frac{\dot{\rho}}{\rho} = -3(1+w)\frac{\dot{a}}{a} \implies \rho \propto a^{-3(1+w)}. \quad (23)$$

This means that the energy density of different kinds of fluids scales down with the expansion of the universe with different powers of the scale factor:

$$\begin{aligned} \text{radiation: } w = 1/3 &\implies \rho \propto a^{-4} \\ \text{dust: } w = 0 &\implies \rho \propto a^{-3} \\ \text{vacuum energy: } w = -1 &\implies \rho \propto \text{const.} \end{aligned}$$

The phases of the universe where the radiation/matter/vacuum energy are the dominant components are called radiation domination (RD), matter domination (MD) and vacuum energy domination, respectively.

Another argument to reach the same conclusions is to consider that the rest-mass energy must be a constant quantity unaffected by the expansion; the volume scales like a^3 in the expanding universe. So the energy density (energy per unit volume) of matter should scale like a^{-3} . For radiation, the energy density has a further $1/a$ factor due to the redshift, so a^{-4} .

2.2.3 Friedmann Equation

The (00) component of the Einstein equations for the FRW metric with parameter k gives the Friedmann Equation

$$H^2 = \frac{8\pi G_N}{3}\rho - \frac{k}{a^2} + \frac{\Lambda}{3}, \quad (24)$$

where the Hubble parameter $H \equiv \dot{a}/a$ is not a constant. The (ii) component of the Einstein equations

$$\frac{\ddot{a}}{a} = -\frac{4\pi G_N}{3}(\rho + 3p) + \frac{\Lambda}{3} \quad (25)$$

does not add anything new with respect to the combination of the Friedmann Equation (24) and the conservation law (20).

So, the system of equations

$$H^2 = \frac{8\pi G_N}{3}\rho_{\text{tot}} - \frac{k}{a^2}, \quad (26)$$

$$\dot{\rho} + 3H(\rho + p) = 0, \quad (27)$$

where

$$\rho_\Lambda \equiv \frac{\Lambda}{8\pi G_N}, \quad (28)$$

is the cosmological constant energy density and

$$\rho_{\text{tot}} \equiv \rho + \rho_\Lambda, \quad (29)$$

is the total energy density, encodes the evolution of the universe and its constituents. The so-called ‘‘curvature energy density’’, encoded in the term proportional to k is also sometimes indicated as $\rho_k = -3k/(8\pi G_N a^2)$.

2.2.4 Cosmological Dynamics

Let us first introduce a notation which is often used in cosmology. The ‘‘critical’’ energy density is defined as

$$\rho_c \equiv \frac{3H^2}{8\pi G_N}, \quad (30)$$

which today is $\rho_c \simeq 1.88 \times 10^{-29} h^2 \text{g cm}^{-3}$ or $\rho_c \simeq 1.05 \times 10^{-5} h^2 \text{GeV cm}^{-3}$. The energy density today of each component is normalized to the critical density to provide the corresponding ‘‘Omega parameter’’ for matter, radiation, curvature and cosmological constant

$$\Omega_m \equiv \frac{\rho_m}{\rho_c}, \quad (31)$$

$$\Omega_r \equiv \frac{\rho_r}{\rho_c}, \quad (32)$$

$$\Omega_k \equiv \frac{\rho_k}{\rho_c} = -\frac{k}{a^2 H^2}, \quad (33)$$

$$\Omega_\Lambda \equiv \frac{\rho_\Lambda}{\rho_c} = \frac{\Lambda}{3H^2}. \quad (34)$$

In terms of the Omega parameters, the Friedmann equation (26) can be simply written as a sum rule

$$\Omega_m + \Omega_r + \Omega_\Lambda + \Omega_k = 1. \quad (35)$$

Now we have all the tools to study the time evolution of the scale factor of the universe. Let us carry out the case where the universe is filled by a single fluid, either matter dust ($w = 0$), radiation ($w = 1/3$) or vacuum energy ($w = -1$). The Friedmann Equation can be written as

$$\left(\frac{\dot{a}}{a}\right)^2 = H_0^2 \left(\frac{\dot{a}}{a_0}\right)^{-3(1+w)}, \quad (36)$$

where $_0$ subscripts indicate present-time quantities. By introducing the new variable $y \equiv a/a_0$, a simple manipulation gives

$$\dot{y} = H_0 y^{1-\frac{3(1+w)}{2}} \implies y^{\frac{1}{2}+\frac{3}{2}w} dy = H_0 dt, \quad (37)$$

which in turns leads to

$$a(t) \propto t^{\frac{2}{3(1+w)}} \quad (w \neq -1), \quad (38)$$

$$a(t) \propto e^{H_0 t} \quad (w = -1), \quad (39)$$

So in a vacuum-dominated universe the scale factor expands exponentially, while in a radiation-dominated (RD) or matter-dominated (MD) phase the expansion is power-law, with exponents

$$a(t) \propto t^{2/3} \quad (w = 0, \text{MD}), \quad (40)$$

$$a(t) \propto t^{1/2} \quad (w = 1/3, \text{RD}). \quad (41)$$

From the Friedmann equation it follows that the total energy density of the universe equals the critical energy density if and only if the FRW parameter $k = 0$, which means the universe is flat

$$\rho_{\text{tot}} = \rho_c \iff k = 0 \iff \text{Flat universe}. \quad (42)$$

2.2.5 Energy Budget

The picture emerging from Cosmic Microwave Background (CMB) measurements performed by PLANCK in 2018 [1] is

$$h = 0.6736 \pm 0.0054 \quad (43)$$

$$\Omega_m h^2 = 0.1430 \pm 0.0011 \quad \begin{cases} \Omega_b h^2 = 0.02237 \pm 0.00015 \\ \Omega_{\text{CDM}} h^2 = 0.1200 \pm 0.0012 \end{cases} \quad (44)$$

$$\Omega_k h^2 = 0.0007 \pm 0.0019 \quad (45)$$

$$\Omega_\Lambda = 0.6847 \pm 0.0073 \quad (46)$$

So the curvature term is consistent with 0% of the energy budget (our Universe is flat!), while non-relativistic matter contributes to about 32% of the budget (split into 5% of ordinary baryonic matter and 27% of unknown dark matter), while the remaining 68% of the energy density of the present universe is in the form of unknown vacuum energy. In summary, we only know the nature of the 5% of what surrounds us.

2.2.6 Age of the universe

Very early (uncertain) times give an almost irrelevant contribution to the age of the universe, so we can compute the age of the universe from when it started RD or MD eras. Start with the definition of the Hubble parameter

$$\frac{da}{dt} = H a, \quad (47)$$

and the Friedmann equations written in terms of Ω 's

$$H(a)^2 = H_0^2 \left[\Omega_r \left(\frac{a_0}{a} \right)^4 + \Omega_m \left(\frac{a_0}{a} \right)^3 + \Omega_k \left(\frac{a_0}{a} \right)^2 + \Omega_\Lambda \right]. \quad (48)$$

From the two equations above it follows that

$$dt = \frac{da}{aH_0} \frac{1}{\left[\Omega_r \left(\frac{a_0}{a} \right)^4 + \Omega_m \left(\frac{a_0}{a} \right)^3 + \Omega_k \left(\frac{a_0}{a} \right)^2 + \Omega_\Lambda \right]^{1/2}}. \quad (49)$$

The estimate of the age of the universe is $t \simeq 13 \text{ Gyrs} = 1.3 \times 10^{10} \text{ yrs}$.

In an MD universe ($\Omega_r = \Omega_k = \Omega_\Lambda = 0, \Omega_m = 1$) Eq. (49) gives

$$t_0 = \frac{2}{3} \frac{1}{H_0} \simeq 9 \times 10^9 \text{ yrs}, \quad (50)$$

which is too young. By allowing a 70% contribution from vacuum energy, as suggested by Eq. (46): $\Omega_r = \Omega_k = 0, \Omega_m = 1 - \Omega_\Lambda = 0.3$, Eq. (49) can be integrated as

$$t = \frac{2}{3} \frac{1}{H_0 \sqrt{\Omega_\Lambda}} \sinh^{-1} \sqrt{\frac{\Omega_\Lambda}{1 - \Omega_\Lambda} \left(\frac{a}{a_0} \right)^3}, \quad (51)$$

so the present age of the universe would be

$$t_0 = \frac{2}{3} \frac{1}{H_0 \sqrt{\Omega_\Lambda}} \sinh^{-1} \sqrt{\frac{\Omega_\Lambda}{1 - \Omega_\Lambda}} \simeq 1.3 \times 10^{10} \text{ yrs}, \quad (52)$$

in perfect agreement with the estimate. The contribution of Λ makes the universe older.

2.2.7 Distance-Redshift Relation

The light rays travel along geodesics defined by $ds = 0$, so in the FRW metric (13) with $k = 0$ the trajectory of light rays is $\theta = \text{const.}$, $\phi = \text{const.}$ and $dr = dt/a$. Using dt from the definition of $H = (1/a)da/dt$, we get

$$dr = \frac{da}{a^2 H}, \quad (53)$$

which combined with Eq. (48) gives

$$r(a) = \frac{1}{H_0} \int_a^{a_0} \frac{da'}{a'^2 \left[\Omega_r \left(\frac{a_0}{a'} \right)^4 + \Omega_m \left(\frac{a_0}{a'} \right)^3 + \Omega_k \left(\frac{a_0}{a'} \right)^2 + \Omega_\Lambda \right]^{1/2}}. \quad (54)$$

This equation is immediately rewritten in terms of the redshift $1 + z = a_0/a$, to get the distance-redshift relation

$$r(z) = \frac{1}{H_0} \int_0^z \frac{dz'}{\left[\Omega_r (1 + z')^4 + \Omega_m (1 + z')^3 + \Omega_k (1 + z')^2 + \Omega_\Lambda \right]^{1/2}}, \quad (55)$$

which allows to infer the distance of an object of known redshift z , depending on the energy content of the universe.

It is convenient also to introduce the *luminosity distance* d_L of an object of given luminosity, from the definition of the flux of photons received from the object

$$\text{Flux} = \frac{\text{Luminosity}}{4\pi r(z)^2 (1 + z)^2} \equiv \frac{\text{Luminosity}}{4\pi d_L^2} \quad (56)$$

so $d_L \equiv (1 + z)r(z)$, which again depends on the universe content. The two powers of $(1 + z)$ in the denominator are originated from the redshift of the energy and the relativistic dilation of time.

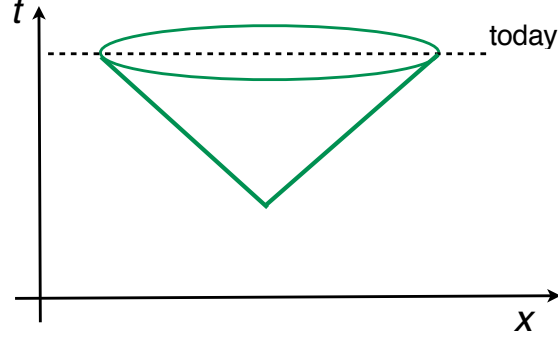


Fig. 2: Particle horizon.

2.2.8 Particle Horizon

A very important concept in cosmology is the notion of particle horizon. It is defined as the boundary between the visible universe and the part of the universe from which light signals have not reached us

$$d_H(t) = a(t) \int_0^t \frac{dt'}{a(t')}. \quad (57)$$

So the particle horizon measures the portion of the universe in causal contact with us (see Fig. 2). Eq. (57) can be re-written using $dt = da/(aH)$ and the expression for H as in Eq. (48), so

$$d_H(t) = \frac{a(t)}{H_0} \int_0^{a(t)} \frac{da'}{a'^2 \left[\Omega_r \left(\frac{a_0}{a'} \right)^4 + \Omega_m \left(\frac{a_0}{a'} \right)^3 + \Omega_k \left(\frac{a_0}{a'} \right)^2 + \Omega_\Lambda \right]^{1/2}}, \quad (58)$$

The special cases of matter-, radiation- and vacuum-domination are particularly interesting

$$d_H(t) = 3t = \frac{2}{H(t)} \propto a^{3/2} \quad (\text{MD}), \quad (59)$$

$$d_H(t) = 2t = \frac{1}{H(t)} \propto a^2 \quad (\text{RD}), \quad (60)$$

$$d_H(t) = \infty, \quad (61)$$

so particle horizon is growing with powers of the scale factors in MD and RD universes while there is no horizon in a universe dominated by vacuum energy.

2.2.9 Equilibrium Thermodynamics

It is useful for future developments to collect some formulae related to the equilibrium thermodynamics of the universe. Let us consider a particle species A with g_A degrees of freedom and chemical potential μ_A , and characterized by a phase space distribution function $f_a(\mathbf{p})$ in momentum space, and energy $E(\mathbf{p})$. The distribution function of a species A takes the form

$$f_A(\mathbf{p}) = \frac{1}{e^{(E(\mathbf{p})-\mu_A)/T} \mp 1}, \quad E(\mathbf{p}) = \sqrt{|\mathbf{p}|^2 + m_A^2} \quad (62)$$

with $-(+)$ for Bose-Einstein (Fermi-Dirac) statistics, respectively. The equilibrium number density and energy density are given by

$$n_A^{\text{eq}} = \frac{g_A}{(2\pi)^3} \int f(\mathbf{p}) d^3 p, \quad (63)$$

$$\rho_A^{\text{eq}} = \frac{g_A}{(2\pi)^3} \int E(\mathbf{p}) f(\mathbf{p}) d^3 p. \quad (64)$$

In extreme cases these integrals can be solved analytically.

For non-relativistic species (whose mass is much greater than the temperature $T \ll m_A$), the above expressions simplify to

$$n_A^{\text{eq}} = g_A \left(\frac{m_A T}{2\pi} \right)^{3/2} e^{-(m_A - \mu_A)/T} \quad (65)$$

$$\rho_A^{\text{eq}} = n_A^{\text{eq}} \cdot m_A. \quad (66)$$

Notice that these quantities are exponentially suppressed by the large mass of the species.

In the opposite regime of ultra-relativistic species ($T \gg m_A, \mu_A$), the expressions depend on the statistics. The number density (at equilibrium) is

$$n_A^{\text{eq}} = \frac{\zeta(3)}{\pi^2} g_A T^3 \begin{cases} 1 & (\text{bosons}) \\ \frac{3}{4} & (\text{fermions}) \end{cases}. \quad (67)$$

The Riemann zeta function of 3 is $\zeta(3) \equiv \sum_{n=1}^{\infty} (1/n^3) \simeq 1.20206$. The energy density (at equilibrium) is

$$\rho_A^{\text{eq}} = \frac{\pi^2}{30} g_A T^4 \begin{cases} 1 & (\text{bosons}) \\ \frac{7}{8} & (\text{fermions}) \end{cases}. \quad (68)$$

Because of the suppression in the non-relativistic regime, the energy density at given temperatures is exponentially dominated by the degrees of freedom which are ultra-relativistic at that temperature. For a collection of several particle species in equilibrium where the species i has thermal distribution with temperature T_i , to a very good approximation the total energy density is

$$\rho_{\text{tot}} = \frac{\pi^2}{30} g_*(T) T^4, \quad (69)$$

where $g_*(T)$ is the total number of relativistic (massless) degrees of freedom at temperature T given by

$$g_*(T) = \sum_{b \in \text{bosons}} g_b \left(\frac{T_b}{T} \right)^4 + \frac{7}{8} \sum_{f \in \text{fermions}} g_f \left(\frac{T_f}{T} \right)^4. \quad (70)$$

The Hubble rate in the RD era (where $a(t) \propto \sqrt{t}$ so $H = 1/(2t)$) can thus be written as

$$H^2 = \frac{8\pi G_N}{3} \rho_{\text{tot}} = \frac{8\pi G_N}{3} \frac{\pi^2}{30} g_*(T) T^4 \simeq 1.66 \sqrt{g_*(T)} \frac{T^2}{M_P}, \quad (71)$$

hence, we obtain the time-temperature relation

$$t \simeq \frac{0.30}{\sqrt{g_*(T)}} \frac{M_P}{T^2} \simeq \frac{2.41}{\sqrt{g_*(T)}} \left(\frac{\text{MeV}}{T} \right)^2 \text{ s}. \quad (72)$$

2.2.10 Temperature-Expansion Relation

The 1st law of thermodynamics relates the change in the energy dU to the change of entropy dS as

$$dU + p dV = T dS \quad (73)$$

The entropy density s is therefore

$$s(T) \equiv \frac{S(V, T)}{V} = \frac{\rho(T) + p(T)}{T} = \frac{4}{3} \frac{\rho(T)}{T} = \frac{2\pi^2}{45} g_{*,s}(T) T^3 \quad (74)$$

where we have used that $p = 1/3\rho$ for RD and defined the quantity

$$g_{*,s}(T) = \sum_{b \in \text{bosons}} g_b \left(\frac{T_b}{T} \right)^3 + \frac{7}{8} \sum_{f \in \text{fermions}} g_f \left(\frac{T_f}{T} \right)^3, \quad (75)$$

which is similar to $g_*(T)$ in Eq. (70) but with the different temperature dependence. Since the energy density scales like $\rho(T) \propto T^4$, the entropy density scales like

$$s(T) \propto g_{*,s} T^3, \quad (76)$$

and therefore the conservation of the entropy within a comoving volume V in thermal equilibrium gives

$$S(V, T) = s(T)V = \text{const.} \implies g_{*,s} T^3 a^3 = \text{const.} \implies T \propto \frac{1}{g_{*,s}^{1/3} a}. \quad (77)$$

In periods where $g_{*,s}$ is also a constant, the temperature simply scales as the inverse of the scale factor $T \propto 1/a$.

3 Big Bang Nucleosynthesis

Big Bang Nucleosynthesis (BBN) occurs at times $1 \text{ s} \lesssim t \lesssim 10^3 \text{ s}$ or equivalently at temperatures of the universe $1 \text{ MeV} \gtrsim T \gtrsim 10 \text{ keV}$. Before BBN, the photons have sufficiently high energy to prevent the formation of nuclei by dissociating them. As the universe cools down, the nuclei of light elements H, D, ^3He , ^4He , ^7Li , get produced with predicted abundances in a remarkably good agreement with the observed ones. All elements heavier than ^7Li are produced later in the history of the universe by nuclear reactions in stars or by other astrophysical processes like supernovae.

BBN is the earliest probe of the universe. Before BBN, we do not know anything about the universe. We are not even sure that the universe existed with temperatures above the MeV.

BBN is one of the main successes of standard cosmology. This success has 3 important consequences:

1. it confirms the theory of the early universe;
2. it provides a determination of the baryon-to-photon ratio η ;
3. to avoid spoiling its success, particle physics theories beyond the Standard Model are constrained.

The predictions for abundances of light elements span 9 orders of magnitude and are all well fitted by a single parameter: the baryon-to-photon ratio $\eta \equiv n_B/n_\gamma$ (see Figure 3). This is one of the greatest successes of Standard Cosmology.

The measurement of light element abundances implies a measurement of η and hence a measurement for Ω_b today. In fact, the energy density in baryons (non-relativistic particles with mass equal to the nucleon mass m_N) can be written as

$$\Omega_b h^2 = \frac{m_N n_B}{\rho_c / h^2} = \eta \frac{m_N n_\gamma}{\rho_c / h^2} = \frac{\eta}{2.74 \times 10^{-8}}. \quad (78)$$

From BBN $0.019 \leq \Omega_b h^2 \leq 0.024$, in good agreement with the independent measurement from CMB (see Eq. (44)). These values are consistent with $\eta \simeq 6 \times 10^{-10}$.

Therefore, together with the measurement of Ω_m from CMB, BBN predicts that $\Omega_b < \Omega_m$, thus providing a compelling argument for the existence of a non-baryonic matter component of the universe, called Dark Matter (DM).

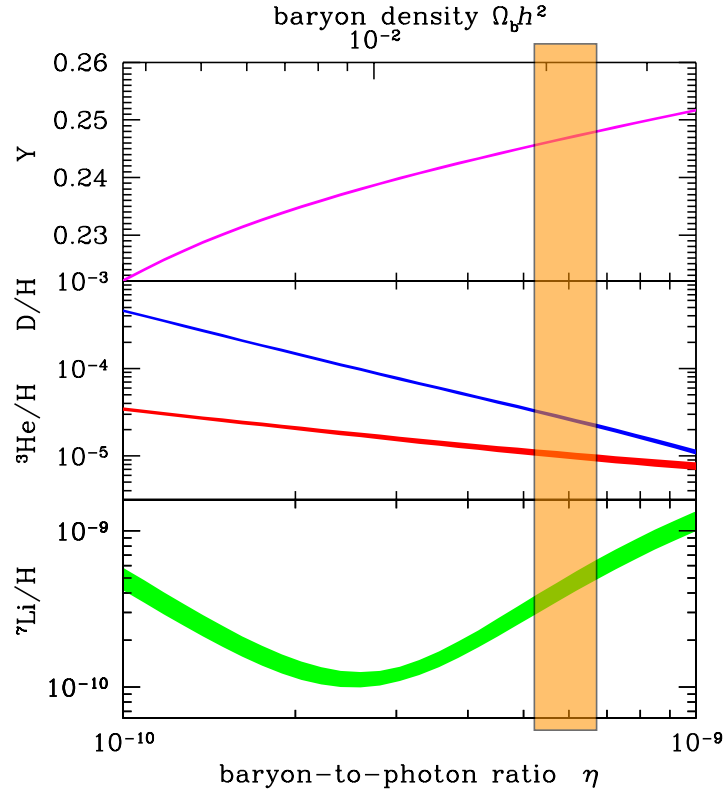


Fig. 3: BBN predictions for light elements abundances. (adapted from Ref. [2])

3.1 Helium fraction

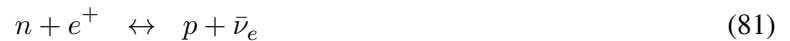
As an example, let us see how much Helium-4 is produced during BBN. We will be deliberately oversimplifying the discussion, for simplicity. For a more general and complete treatment of the BBN dynamics see e.g. the excellent textbooks in Refs. [3–5].

Observations of metal-poor stars and gas clouds provide an experimental determination of the abundance of ${}^4\text{He}$ nuclei with respect to the total number of baryons (protons + neutrons) as

$$Y \equiv \frac{4n_{\text{He}}}{n_n + n_p} \simeq 0.24. \quad (79)$$

So, in order to compute Y we need to compute n_n/n_p and n_{He}/n_p .

At very early times ($T \gg 1$ MeV, $t \ll 1$ s), there are only protons and neutrons which are kept in equilibrium by the reactions



so $n_n = n_p$. When these reactions are in equilibrium, they enforce the balance of chemical potentials as

$$\mu_n + \mu_{\nu_e} = \mu_p + \mu_e. \quad (83)$$

Since the chemical potentials of electrons and neutrinos are negligibly small, we can conclude that $\mu_n = \mu_p$. At MeV temperatures neutrons and protons are non-relativistic, and their mass difference starts to be

important. So, recalling the equilibrium number densities for non-relativistic species Eq. (65) we obtain the neutron-to-proton ratio (in equilibrium) as

$$\frac{n_n^{\text{eq}}}{n_p^{\text{eq}}} = \frac{g_n}{g_p} \left(\frac{m_n}{m_p} \right)^{3/2} e^{-Q/T} e^{(\mu_n - \mu_p)/T} \simeq e^{-Q/T}, \quad (84)$$

where the neutron-proton mass difference is

$$Q = m_n - m_p \simeq 1.29 \text{ MeV}. \quad (85)$$

and we have used that $m_n \simeq m_p$, $\mu_n = \mu_p$ and $g_n = g_p = 2$. The equilibrium is broken by expansion as temperature goes down. The total scattering rate of the reactions involving neutrons and protons is

$$\Gamma = \Gamma(n + \nu_e \leftrightarrow p + e^-) + \Gamma(n + e^+ \leftrightarrow p + \bar{\nu}_e) \simeq 0.96 \left(\frac{T}{\text{MeV}} \right)^5 \text{ s}^{-1}, \quad (86)$$

while the Hubble parameter during radiation domination at $T \lesssim 1 \text{ MeV}$ is

$$H \simeq 1.66 \sqrt{10.75} \frac{T^2}{M_P} \simeq 0.68 \left(\frac{T}{\text{MeV}} \right)^2 \text{ s}^{-1}. \quad (87)$$

Therefore, the comparison of the scattering rate with the expansion rate gives

$$\frac{\Gamma}{H} \simeq \left(\frac{T}{0.8 \text{ MeV}} \right)^3. \quad (88)$$

So at $T \gtrsim 0.8 \text{ MeV}$, the neutron-to-proton ratio follows its equilibrium value, while at $T \lesssim 0.8 \text{ MeV}$ it decouples and freezes out at a value

$$\frac{n_n}{n_p}(T \lesssim 0.8 \text{ MeV}) = \frac{n_n^{\text{eq}}}{n_p^{\text{eq}}}(T = 0.8 \text{ MeV}) = e^{-1.29/0.8} \simeq 0.2 \quad (89)$$

and correspondingly the neutron fraction is

$$X_n(T \lesssim 0.8 \text{ MeV})|_{\text{before decay}} \equiv \frac{n_n}{n_n + n_p} = \frac{\frac{n_n}{n_p}}{1 + \frac{n_n}{n_p}} \simeq \frac{e^{-1.29/0.8}}{1 + e^{-1.29/0.8}} \simeq 0.17. \quad (90)$$

After that time, some neutrons decay ($\tau_n \simeq 886 \text{ s}$) and at later time, at the onset of BBN, $T_D \simeq 70 \text{ keV}$ (the temperature at which deuterium production becomes thermodynamically favoured), there are slightly fewer neutrons. The time-temperature relation in the temperature regime $T < T_D$ is obtained from Eq. (72), with $g_* = 3.36$ (after e^\pm annihilations),

$$t(T) \simeq 1.32 \left(\frac{1 \text{ MeV}}{T} \right)^2 \text{ s}, \quad (91)$$

and therefore the neutron fraction at late times is

$$X_n(T < T_D) = X_n|_{\text{before decay}} \times e^{-t(T_D)/\tau_n} \simeq 0.12, \quad (92)$$

leading to the neutron-to-proton ratio

$$\frac{n_n}{n_p}(T < T_D) \simeq 0.14. \quad (93)$$

Next, we need the number density of Helium nuclei n_{He} . Helium-4 is not produced by direct synthesis of $2n$ and $2p$, as the corresponding reaction rates are highly suppressed in the dilute (high entropy) limit,

but rather by burning of deuterium ${}^2H = D$. So, in order to produce 4He one needs to “wait” until the D is produced, which occurs relatively late, because of the small binding energy of D (the so-called “deuterium bottleneck”). Only after D is formed, it can be burnt by the reactions



and then provide the fuel for Helium-4 production



Deuterium is formed by the direct synthesis of one neutron and one proton in the reaction



The D production becomes efficient at temperatures $T \lesssim T_D \simeq 70$ keV, and nearly all free neutrons get bound into Helium-4 nuclei, so

$$n_{{}^4He} \simeq n_n/2, \quad (99)$$

since each Helium-4 nucleus contains two neutrons. Now we have all the ingredients to estimate the 4He abundance produced by BBN, by combining Eqs. (93) and (99)

$$Y = \frac{4n_{{}^4He}}{n_n + n_p} = \frac{4n_n/2}{n_n + n_p} = \frac{2n_n/n_p}{1 + n_n/n_p} \simeq 0.24, \quad (100)$$

in very good agreement with the observed value.

4 Cosmic Microwave Background

In 1965 Arno Penzias and Robert Wilson published a paper where they admitted to have failed to eliminate a background noise coming from all directions, corresponding to a residual photon background with temperature of about 3 K. Ten years later they shared the Nobel prize in physics for the discovery of the Cosmic Microwave Background (CMB) radiation!

What was that noise?

At temperatures above the electron mass m_e ($T > m_e$) the electrons/positrons and radiation were in thermal equilibrium. When the temperature of the universe goes down to a fraction of the electron mass ($T \lesssim m_e$), electrons and positrons become non-relativistic and their equilibrium number densities become exponentially suppressed compared to the number density of photons, so the reaction



goes out of equilibrium and chemical equilibrium is broken. However, matter (residual electrons) and radiation are still in kinetic equilibrium, through the elastic reaction (Compton scattering)



whose cross section for non-relativistic electrons reduces to the Thomson scattering cross section (in classical electrodynamics)

$$\sigma_T \simeq \frac{8\pi}{3} \left(\frac{\alpha}{m_e} \right)^2 \simeq 6.7 \times 10^{-25} \text{ cm}^2. \quad (103)$$

Notice that the analogous Compton scattering of photons off protons $p\gamma \leftrightarrow p\gamma$ is irrelevant since the corresponding cross section is suppressed by $(m_e/m_p)^2 \sim 10^{-6}$. The Compton scattering keeps the

photons coupled to matter until a much later time (photon decoupling) than when $T \simeq m_e$. Until then, kinetic equilibrium is attained and photons are continuously scattering off electrons. The universe was filled with an almost perfect black-body radiation.

When Compton scatterings start becoming ineffective with respect to the expansion rate of the universe, the photons “decouple” from matter and then propagate freely until today. They just cooled with expansion down to a temperature $T_0 = 2.7 \text{ K} = 2.3 \times 10^{-4} \text{ eV}$. This radiation is the residual electromagnetic radiation from the Big Bang, observed as a highly isotropic “noise”. The CMB can therefore be interpreted as a snapshot of the universe when it was very young (about 300,000 yrs old, as we will see later). The CMB provides a huge deal of information about our universe, and it is the most powerful cosmological probe available today.

4.1 Photon energy density

The energy distribution of thermal photons follows the Planck distribution (let us restore the units of c, \hbar, k_B in this subsection)

$$n(\omega, T)d\omega = \frac{1}{c^3} \frac{1}{e^{\hbar\omega/(k_B T)} - 1} \frac{2d^3\omega}{(2\pi)^3} = \frac{1}{\pi^2 c^3} \frac{\omega^2 d\omega}{e^{\hbar\omega/(k_B T)} - 1} \quad (104)$$

the differential energy spectrum

$$u(\omega, T)d\omega = (\hbar\omega)n(\omega, T)d\omega = \frac{\hbar}{\pi^2 c^3} \frac{\omega^3 d\omega}{e^{\hbar\omega/(k_B T)} - 1} \quad (105)$$

is the usual one for a black body. Therefore the total energy density in radiation is given by the integral

$$\rho_\gamma = \int_0^\infty u(\omega, T)d\omega = \frac{\hbar}{\pi^2 c^3} \left(\frac{k_B T}{\hbar} \right)^4 \int_0^\infty \frac{\xi^3 d\xi}{e^\xi - 1} = \frac{\pi^2 k_B^4}{15 \hbar^3 c^3} T^4 \equiv \sigma T^4 \quad (106)$$

with $\sigma = 4.72 \times 10^{-3} \text{ eV cm}^{-3} \text{ K}^{-4}$ being the Stefan-Boltzmann constant. This energy density today ($T=2.7 \text{ K}$) is $\rho_\gamma \simeq 0.26 \text{ eV cm}^{-3}$, which translates into

$$\Omega_r h^2 = \frac{\rho_\gamma}{\rho_c / h^2} \simeq 4 \times 10^{-5}, \quad (107)$$

so the present radiation energy density is negligible.

4.2 Photon decoupling

Let us compute the time when the CMB formed (or equivalently the redshift of photon decoupling z_{dec}). We will work under the simplifying approximation that the plasma is in chemical and thermal equilibrium among all its components, aiming at providing the reader with the basic elements. For more exhaustive discussions please refer e.g. to Refs. [4, 5].

The goal is to estimate the time of *photon decoupling*, namely when the photons stop interacting with matter and propagate through the universe along geodesics. We first need to find the number density of free electrons, or equivalently the free electron fraction (or ionization fraction)

$$X_e \equiv \frac{n_e}{n_p + n_H}. \quad (108)$$

Free electrons get bound to protons to form neutral H atoms through the capture reaction



and the binding energy of H is

$$B_H \equiv m_e + m_p - m_H = 13.6 \text{ eV}. \quad (110)$$

When $T \ll m_e$, electrons, protons and Hydrogen atoms are non-relativistic and their equilibrium number densities are given by Eq. (65)

$$n_i^{\text{eq}} = g_i \left(\frac{m_i T}{2\pi} \right)^{3/2} e^{-(m_i - \mu_i)/T}, \quad (i = e, p, H), \quad (111)$$

and recall that $g_p = g_e = 2$. The first type of Hydrogen involved in the electron capture in Eq. (109) is H_{1s} , i.e. the ground state (with 2 hyperfine states, one with spin 0 and one with spin 1, so $g_{H_{1s}} = 1 + 3 = 4$). By adding to the 3 conditions for n_i^{eq} the 3 relations following from the equilibrium reaction in Eq. (109)

$$\begin{cases} \mu_p + \mu_e = \mu_H & \text{(chemical equilibrium)} \\ n_e = n_p & \text{(charge neutrality)} \\ n_p + n_H = 0.76 n_B = 0.76 \eta n_\gamma & \text{(tot. number of baryons without } He) \end{cases} \quad (112)$$

(recall that after BBN about 24% of the baryons consists of ${}^4\text{He}$) we have 6 equations for the 6 unknowns $n_{p,e,H}, \mu_{p,e,H}$. We can then compute, in the equilibrium approximation, the quantity

$$\begin{aligned} \left. \frac{X_e^2}{1 - X_e} \right|_{\text{eq}} &= \frac{n_e^{\text{eq}} + n_H^{\text{eq}}}{n_H^{\text{eq}}} \frac{n_e^{\text{eq}} n_p^{\text{eq}}}{(n_e^{\text{eq}} + n_H^{\text{eq}})^2} = \frac{n_e^{\text{eq}} n_p^{\text{eq}}}{n_H^{\text{eq}} (n_e^{\text{eq}} + n_H^{\text{eq}})} = \frac{1}{0.76 \cdot \eta n_\gamma} \frac{n_e^{\text{eq}} n_p^{\text{eq}}}{n_H^{\text{eq}}} \\ &= \frac{1}{0.76 \cdot \eta n_\gamma} \frac{g_e g_p}{g_H} \left(\frac{m_e T}{2\pi} \right)^{3/2} e^{(\mu_e + \mu_p - \mu_H)/T} e^{-(m_e + m_p - m_H)/T} \\ &= \frac{1}{0.76 \cdot \eta n_\gamma} \left(\frac{m_e T}{2\pi} \right)^{3/2} e^{-B_H/T}. \end{aligned} \quad (113)$$

Inserting $n_\gamma^{\text{eq}} = (2/\pi^2)\zeta(3)T^3$, we get the *Saha equation* for the equilibrium ionization fraction of electrons

$$\left. \frac{X_e^2}{1 - X_e} \right|_{\text{eq}} = \frac{\sqrt{\pi}}{0.76 \cdot 4\sqrt{2}\zeta(3)\eta} \frac{1}{T} \left(\frac{m_e}{T} \right)^{3/2} e^{-B_H/T}. \quad (114)$$

The latter equation can be solved in the two temperature regimes

$$T \gtrsim B_H \implies \left. \frac{X_e^2}{1 - X_e} \right|_{\text{eq}} \simeq 10^9 \left(\frac{m_e}{T} \right)^{3/2} \simeq 10^5 \implies X_e \simeq 1 \quad (\text{all H ionized}) \quad (115)$$

$$T < B_H \implies X_e^{\text{eq}} \ll 1 \implies X_e^{\text{eq}}(T) \simeq \left[\frac{\sqrt{\pi}}{0.76 \cdot 4\sqrt{2}\zeta(3)\eta} \frac{1}{T} \left(\frac{m_e}{T} \right)^{3/2} e^{-B_H/T} \right]^{1/2}. \quad (116)$$

Now that we have an expression for the free electron fraction at late times, we can proceed to compute the time of photon decoupling.

Photon decoupling occurs when the rate of photon-electron (Compton) scattering is less than the expansion rate: $\Gamma_e \simeq n_e \sigma_T \lesssim H$. Assume for simplicity a matter-dominated universe with $\Omega_m = 1$ (but generalizations are straightforward), so

$$H(T) \simeq H_0 a^{-3/2} = H_0 \left(\frac{T}{T_0} \right)^{3/2}. \quad (117)$$

Then

$$n_e = X_e n_B, \quad (118)$$

$$n_B = \frac{\Omega_b \rho_c}{m_p} \left(\frac{a_0}{a}\right)^3 = \frac{\Omega_b \rho_c}{m_p} \left(\frac{T}{T_0}\right)^3 \simeq 2.2 \times 10^{-7} \text{ cm}^{-3} \left(\frac{T}{T_0}\right)^3, \quad (119)$$

from which it follows that the rate for electron Compton scatterings is

$$\Gamma_e(T) = n_e \sigma_T \simeq X_e 1.5 \times 10^{-31} \text{ cm}^{-1} \left(\frac{T}{T_0}\right)^3. \quad (120)$$

Then compare Γ_e with H from Eq. (117), to get the temperature T_{dec} at which they are equal (recall $H_0^{-1} = 9.3 \times 10^{27} \cdot h^{-1} \text{ cm}$, $h \simeq 0.7$)

$$\Gamma_e(T_{\text{dec}}) = H(T_{\text{dec}}) \implies \left(\frac{T_{\text{dec}}}{T_0}\right)^{3/2} \simeq \frac{1}{2 \times 10^{-3} X_e(T_{\text{dec}})}, \quad (121)$$

and then solve numerically the implicit equation for T_{dec} , where $X_e(T)$ is given by the Saha equation in Eq. (116), arriving at

$$\begin{aligned} T_{\text{dec}} &\simeq 1000 T_0 \simeq 0.2 \text{ eV} \implies 1 + z_{\text{dec}} = \frac{T_{\text{dec}}}{T_0} \simeq 1000 \\ &\implies t_{\text{dec}} = \frac{2}{3H_0(1+z_{\text{dec}})^{3/2}} \simeq 300\,000 \text{ yrs.} \end{aligned} \quad (122)$$

This is the time of photon decoupling (last scattering), when the CMB is formed. Before photon decoupling the plasma is opaque, because of photons scattering off free electrons. After decoupling, photons do not scatter anymore and the universe becomes transparent to radiation.

If instead of the Hubble parameter given by Eq. (117) for $\Omega_m = 1$ one considers a more realistic ΛCDM model where $\Omega_m = 0.27$, $\Omega_\Lambda = 1 - \Omega_m$, one gets $z_{\text{dec}} \simeq 1089$, so $T_{\text{dec}} \simeq 0.26 \text{ eV}$.

4.3 Concluding remarks

The CMB is actually not perfectly isotropic. There are temperature anisotropies of the order of

$$\frac{\Delta T}{T} \sim 10^{-5}. \quad (123)$$

Indeed, these anisotropies carry a great deal of cosmological information. For example, the two-point correlation functions of the temperature maps crucially depend on the cosmological parameters like $H_0, \Omega_b, \Omega_{\text{tot}}$ etc. By a careful analysis of these anisotropies, satellite experiments like COBE, WMAP and lately PLANCK were able to determine the cosmological parameters with greater and greater accuracy. The CMB anisotropies in the CMB are well described by acoustic oscillations in the photon-baryon plasma. Both ordinary baryonic and dark matter interact gravitationally with radiation, but only ordinary matter interacts also electromagnetically. So baryonic and dark matter affect the CMB differently. From the peaks of the CMB it is possible to determine the density of baryonic and dark matter. The resulting best-fit ‘concordance’ cosmological model is known as ΛCDM (cosmological constant plus cold dark matter), where roughly

$$\Omega_{\text{tot}} \sim 1.0, \quad \Omega_{\text{matter}} \sim 0.3, \quad \Omega_{\text{radiation}} \sim 0.0, \quad \Omega_\Lambda \sim 0.7 \quad (124)$$

The accurate determination of the energy content of the universe was another great triumph of standard cosmology!

So, although standard cosmology is very successful at providing a picture of the universe from BBN to today, there are several questions still lacking an answer, for instance: what is the dark matter made of? why there is a matter-antimatter asymmetry? what happened in the first three minutes of the universe (before BBN)? We will discuss some possible answers to these (and other) questions in the remainder of the course.

5 Dark Matter

5.1 Evidences for dark matter

We already discussed that both BBN and CMB observations (see Section 2.2.5) provide compelling arguments in favour of the existence of an unknown component of the universe consisting of non-baryonic matter, dubbed Dark Matter (DM). The existence of DM is by now firmly established also by other types of observational evidences.

5.1.1 Galaxy clusters

- **Coma cluster.** In 1933, F. Zwicky measured the proper motion of galaxies in the Coma galaxy cluster (a group of ~ 1000 galaxies, within a radius of ~ 1 Mpc).

The mass M and the size R of the cluster of N galaxies can be related to the velocity dispersion of galaxies (the velocities are projected along the line of sight) according to the virial theorem:

$$\begin{aligned} \langle V \rangle + 2\langle K \rangle &= 0, \\ \langle V \rangle &= -\frac{N^2}{2}G_N \frac{\langle m^2 \rangle}{R} \quad (\text{average pot energy due to } N^2/2 \text{ pairs of galaxies}), \\ \langle K \rangle &= N \frac{\langle mv^2 \rangle}{2} \quad (\text{average kin energy due to } N \text{ galaxies}). \end{aligned} \quad (125)$$

The total mass M is

$$M = N\langle m \rangle \sim \frac{2R\langle v^2 \rangle}{G_N}, \quad (126)$$

from which it was computed the mass-to-luminosity ratio to be much larger than the one for an average star like the Sun

$$\frac{M}{L} \sim 300h \frac{M_\odot}{L_\odot}. \quad (127)$$

So the value obtained is about 300 times greater than expected from their luminosity, which means that most of the matter is not luminous, so it is dark.

- **X-ray observations.** The gravitational potential (and hence the total mass) of galaxy clusters can also be measured by X-ray observations. In fact, most of the ordinary mass in cluster is in the form of hot gas, emitting X-ray frequencies. The X-rays are produced by electrons.

It is possible to measure the spatial distributions of the electron number density $n_e(r)$ and of the electron temperature $T_e(r)$. The number density of baryons $n_b(r)$ will be proportional to n_e up to a factor μ depending on the chemical composition: $n_b(r) = \mu n_e(r)$. The pressure is mostly due to electrons, so $P(r) = n_e(r)T_e(r)$.

The hydrostatic equilibrium relates the pressure P to the radius R through the mass m which in turn depends on the energy density in baryons ρ_b

$$dP = -dm \frac{\text{acceleration}}{\text{Area}} = -\rho_b(R) \frac{dV}{\text{Area}} \frac{G_N M(R)}{R^2} = -\rho_b(R) \frac{G_N M(R)}{R^2} dR, \quad (128)$$

where the total mass enclosed in a sphere of radius R is

$$M(R) = 4\pi \int_0^R \rho(r) r^2 dr. \quad (129)$$

This leads to

$$\frac{dP}{dR} = -n_b(r) m_b \frac{G_N M(R)}{R^2}. \quad (130)$$

In this equation, the left-hand side is measured from temperature maps from X-ray spectra, the term $n_b(r)$ is obtained from X-ray luminosity and spatial distributions of electrons, so only $M(R)$

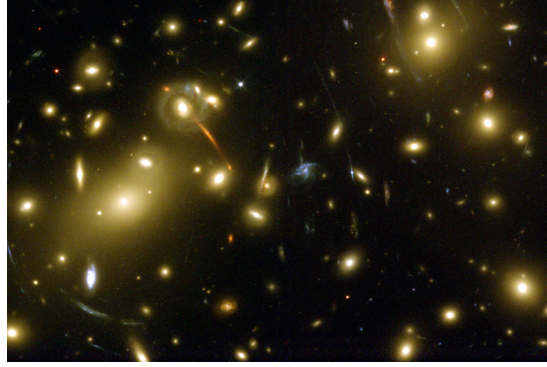


Fig. 4: The gravitational lensing from Abell NGC2218.

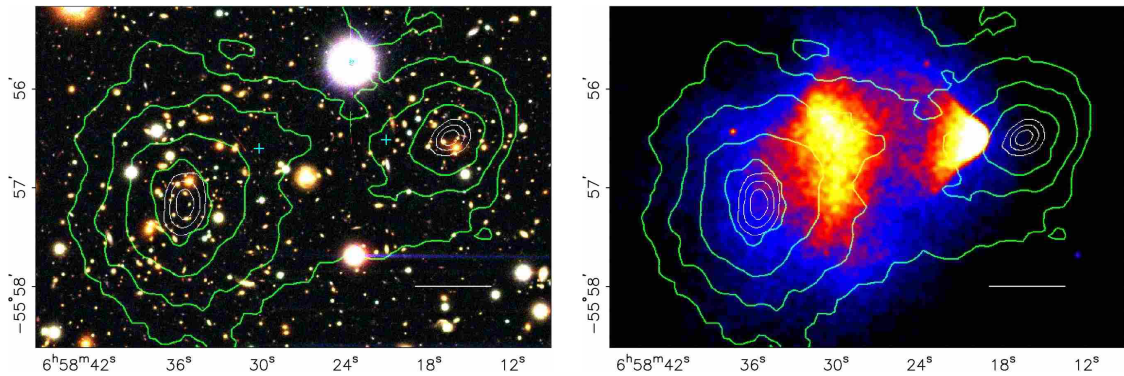


Fig. 5: The “Bullet cluster” 1E0657-558. The image shows two colliding clusters of galaxies. The green lines show the gravitational equipotential surfaces, measured by gravitational lensing. Brighter regions are the hot baryonic gas, observed in X-ray by Chandra. Figure taken from Ref. [6].

is unknown and can be determined. The result for M is again that M should be more than the contribution of just visible (baryonic) matter M_b .

- **Gravitational lensing.** Gravitational lensing techniques use the gravitational distortion of images of distant galaxies due to a gravitational mass (e.g. a cluster) along the line of sight (see Fig. 4). This way, it is possible to reconstruct the gravitational potential, and hence the total mass distribution of the cluster. The result is that more matter than the visible one is required, and also differently distributed.
- **Bullet cluster.** The so-called “bullet cluster” (see Fig. 5) is a recent merging of galaxy clusters. The gravitational potential is not produced by baryons, but by DM. In the collision, the hot gas is collisional and loses energy, so it slows down and lags behind DM; the DM clusters are collisionless and passed through each other.

5.1.2 Galaxies

The dependence of the velocity $v(R)$ of stars in a galaxy, as a function of the distance R from the galactic center (**rotation curves**), is given by Newton’s law (assuming circular motion)

$$v(R) = \sqrt{\frac{G_N M(R)}{R}}, \quad M(R) = 4\pi \int_0^R \rho(r) r^2 dr, \quad (131)$$

where $\rho(r)$ is the mass density. The contribution to ρ from luminous matter would lead to $v(r) \propto R^{-1/2}$ at large R . But observationally, one has $v(R) \simeq \text{constant}$, see Fig. 6. Explaining the observed rotation

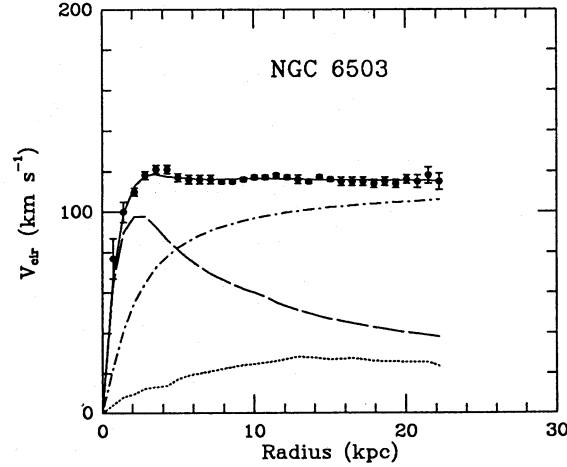


Fig. 6: The rotation curve of galaxy NGC 6503. The different curves show the contribution of the three major components of matter to the gravitational potential (from top to bottom): halo, disk, gas. Figure taken from Ref. [7].

curves requires more matter abundance, and differently distributed, than the visible one: a constant rotation curve requires $M_{\text{DM}} \propto R$, which is attained for a DM density distribution $\rho_{\text{DM}}(r) \propto 1/r^2$.

There exists several other dynamical constraints from studying the motion of stars in the Milky Way. They are then compared to a mass model for the galaxy and allow a determination of the local DM density (at the location of the Sun)

$$\rho(r_{\odot}) \simeq 0.01 M_{\odot} \text{ pc}^{-3} \simeq 0.4 \text{ GeV cm}^{-3} \quad (132)$$

(recall $1 \text{ pc} = 3.08 \times 10^{18} \text{ cm}$, and $1 M_{\odot} = 1.12 \times 10^{57} \text{ GeV}$).

5.1.3 Large-scale structures

Without DM, density perturbations would start to grow only after recombination, so today there would not be structures yet. Different DM types lead to different scenarios for the formation of structures: in the so-called Hot Dark Matter scenario large structures are formed first and then fragment into smaller pieces (“top-down”), while in the Cold Dark Matter scenario smaller objects merge into bigger structures hierarchically (“bottom-up”). Cosmological observations and numerical simulations exclude the Hot DM case.

5.2 Key Properties of Particle DM

A particle candidate for DM must satisfy at least the following fundamental properties:

1. stable, or at least with a lifetime longer than the age of the universe;
2. no electric charge, no color charge;
3. non-collisional, or at least much less collisional than baryons: self-annihilation cross sections must be smaller than QCD $\sigma_{\text{DM DM}} \ll 1/m_p^2$, and weak cross sections $\sigma_{\text{DM DM}} \ll 1/m_Z^2$;
4. not “hot”, as it would be excluded by large-scale structure formation;
5. in the fluid limit, not in the form of a collection of discrete compact objects. We have not seen any discreteness effects in DM halos. Granularities would affect the stability of astrophysical systems. MASSive Compact Halo Objects (MACHOs) are astrophysical objects with macroscopic mass, such as large planets or small dead stars. Searches for MACHOs (EROS+MACHO results) exclude

the range

$$10^{-7}M_{\odot} \lesssim M \lesssim 10M_{\odot}, \quad (133)$$

using gravitational microlensing. Several other constraints also apply, due to e.g. non-observation of lensing effects in the direction of Gamma-Ray Bursts (GRBs) or towards compact radio sources. However, it is natural to expect these objects to be baryonic and created in the late universe. So this would upset predictions for BBN and CMB and they are excluded. A small window for primordial black holes (PBH) is actually still open;

6. non-relativistic (classical) today, in order to be confined on galactic scales (1 kpc or so), for densities $\sim \text{GeV cm}^{-3}$, and velocities $\sim 100 \text{ km s}^{-1}$. This leads to lower limits on its mass, depending on whether DM is made out of bosons or fermions.

- For *bosons*, the De Broglie wavelength $\lambda = h/p$ (h is the Planck's constant, restored in this section) must be less than 1 kpc, so

$$m \gtrsim \frac{h}{1\text{kpc} \cdot v} \simeq 10^{-22} \text{eV}, \quad (134)$$

where $v \simeq 100 \text{ km/s}$ has been used.

- For *fermions*, because of Pauli exclusion principle, the DM quantum occupation number must be smaller than one, so

$$\rho(r_{\odot}) \lesssim \frac{m}{\lambda^3} \implies m \gtrsim \left[\frac{h^3 \rho(r_{\odot})}{v^3} \right]^{1/4} \simeq 1 \text{keV}, \quad (135)$$

where $\rho(r_{\odot}) = 0.4 \text{ GeV cm}^{-3} \simeq (0.04 \text{ eV})^4$ has been used (Gunn-Tremaine bound)

None of the SM particles satisfies the above requirements. Therefore the quest for a viable particle candidate for DM needs to be carried out in the realm of physics beyond the SM.

5.3 Weakly Interacting Massive Particles

There is a really wide landscape of DM models, where the DM mass spans several orders of magnitude, from ultra-light scalars at about 10^{-22} eV to primordial black holes at 10^{20} kg . There is no *a priori* preferred mass scale, so we are not sure where to look for DM.

Among the many possible categorizations of the DM models, one that is particularly useful is to divide the DM candidates into whether or not they are Weakly Interacting Massive Particles (WIMPs). The advantage is that all WIMPs share pretty much the same production mechanism in the early universe, through the so-called thermal *freeze-out*, which we will describe later, while each of the other non-WIMP DM candidates are produced in peculiar ways to be studied case-by-case.

Just to mention a few out of the many realizations of each category, the WIMPs can be the supersymmetric neutralino, minimal DM, Higgs-portal scalar, heavy neutrino, inert Higgs doublet, lightest Kaluza-Klein particle, etc. Some notable non-WIMP candidates are axions, sterile neutrinos, gravitinos, asymmetric DM, techni-baryons, Q-balls, primordial black holes, dark photons, topological defects, etc.

For simplicity, from now on we will only focus on WIMPs. The basic ingredients for a WIMP model are:

- a massive particle in the $\sim 1 \text{ GeV} - \sim 100 \text{ TeV}$ range;
- weak interactions with the SM;
- production via thermal freeze-out in the early universe.

5.4 Freeze-out of Thermal Relics

In this section we want to compute the thermal relic abundance of a particle whose interactions “freeze-out” in the early universe. We will first do a simple estimate, in order to highlight the important quantities into play, then we will describe a more formal calculation using the Boltzmann equations.

Let us start by assuming the Standard Model of particle physics is augmented with the inclusion of a particle χ (the DM) of mass m_χ such that

- χ is a stable;
- χ is coupled to lighter SM species;
- χ is in thermal equilibrium in the early universe at temperature $T \gg m_\chi$.

The DM particle χ is kept in equilibrium by number-changing annihilation processes of the kind

$$\chi \chi \leftrightarrow \text{SM SM}, \quad (136)$$

where SM is any SM particle. This follows from the assumptions 1. and 2. above.

At temperatures much bigger than m_χ , these processes are fast and the DM is in equilibrium with the rest of the plasma. But as the universe expands, the rate for the processes (136) becomes slower than the expansion rate of the universe, and such reactions go out of equilibrium. This happens when the annihilation rate $\Gamma \lesssim H$. From this point on, the DM decouples from the plasma and its number density does not change anymore, it “freezes out”.

Let us find the freeze-out temperature T_f , defined by the condition

$$n_\chi^{\text{eq}}(T_f)\sigma = H(T_f). \quad (137)$$

Let us assume for simplicity here that the annihilation cross section of the process (136) does not depend on the relative velocity: $\sigma = \sigma_0$ (the so-called s -wave annihilation). Now, during radiation domination: $H(T_f) = \sqrt{(4\pi^3/45)g_*(T_f)T_f^2/M_P}$. The equilibrium number density, for $m_\chi \gg T_f$ is

$$n_\chi^{\text{eq}}(T_f) = g_\chi \left(\frac{m_\chi T_f}{2\pi} \right)^{3/2} e^{-m_\chi/T_f}. \quad (138)$$

Eq. (137) can be then manipulated to arrive at an implicit equation for T_f which does not admit closed-form solution, but it can be solved iteratively, giving at leading order

$$T_f \simeq \frac{m_\chi}{\ln K}, \quad (139)$$

where

$$K \equiv \frac{3\sqrt{5}}{4\sqrt{2}\pi^3} \frac{g_\chi}{\sqrt{g_*}} \sigma_0 m_\chi M_P. \quad (140)$$

For reference values $m_\chi = 100 \text{ GeV}$, $g_\chi = 2$, $g_* = 100$ and $\sigma_0 = 1 \text{ pb} = 10^{-36} \text{ cm}^2 \simeq 2.6 \times 10^{-9} \text{ GeV}^{-2}$, we get

$$K = 2.4 \times 10^{10} \left(\frac{g_\chi}{2} \right) \left(\frac{100}{g_*} \right)^{1/2} \left(\frac{\sigma_0}{1 \text{ pb}} \right) \left(\frac{m_\chi}{100 \text{ GeV}} \right) \quad (141)$$

so $\ln K \simeq 24$, and therefore typically $T_f \sim m_\chi/20 \div m_\chi/30$.

Then it follows that the number density of χ at freeze-out is

$$n_\chi(T_f) = \frac{H(T_f)}{\sigma_0} = \sqrt{\frac{4\pi^3}{45} g_*(T_f)} \frac{T_f^2}{M_P} \quad (142)$$

which is roughly constant until today, up to a redshift dilution of non-relativistic matter

$$n_\chi(T_0) = \left(\frac{T_0}{T_f}\right)^3 n_\chi(T_f) \propto \frac{1}{T_f} \propto \frac{1}{m_\chi}. \quad (143)$$

So the energy density today of χ particles is $\rho_\chi(T_0) = n_\chi(T_0)m_\chi$ does not depend on m_χ ! Actually, there is still a mild (logarithmic) residual dependence on m_χ in K .

$$\Omega_\chi h^2 = \frac{\rho_\chi(T_0)}{\rho_c/h^2} = \frac{n_\chi(T_0)m_\chi}{\rho_c/h^2} \simeq 0.1 \frac{3 \times 10^{-26} \text{ cm}^3/\text{sec}}{\sigma_0} \simeq 0.1 \frac{1 \text{ pb}}{\sigma_0} \quad (144)$$

The present relic abundance of χ is mostly driven by its cross section. Notice that a pb cross section is the typical cross section of weak interactions.

Recall from Eq. (44) that the present energy density of DM is observed to be $\Omega_{\text{DM}} h^2 \simeq 0.12$. Therefore, the relic density today of a cold relic produced by the freeze-out mechanism in the early universe can explain the observed value of the DM energy density, as shown by Eq. (144). If σ_0 is bigger than about $10^{-26} \text{ cm}^3/\text{s}$, the relic abundance is too big and would overclose the universe.

A cold relic with weak-scale interactions is a DM candidate. A typical annihilation cross section for a particle with couplings g is $\sigma \sim g^4/M^2$, so a pb cross section is realized by

$$M/g^2 \sim \text{TeV} \quad (145)$$

so the weak scale! A particle of weak-scale mass and couplings gives rise to a relic abundance in the right ballpark of the observed DM abundance. This remarkable coincidence is also known as the ‘‘WIMP miracle’’.

So there are several reasons why the WIMPs are so appealing as DM candidates:

- the WIMP ‘‘miracle’’ (which may just be a numerical coincidence);
- a common production mechanism (freeze-out);
- the link with beyond-the-SM physics at the weak scale, possible related to the solution of the hierarchy problem (e.g. Supersymmetry)
- the possibility to perform multi-sided searches: the three pillars of WIMP searches are the so-called direct detection, indirect detection and collider searches; they may be interpreted as the searches for signatures due to three different realizations of the same WIMP-quark interactions: WIMP-quark scattering, WIMP self-annihilations and WIMP pair production from quarks. In the next subsections we will discuss each of them.

5.5 Direct Detection

Direct Detection (DD) of DM consists of looking for the scatterings of galactic halo DM on heavy nuclei in underground laboratories. Suppose a halo particle χ with mass m_χ and velocity v scatters from a target nucleus at rest of atomic mass number A and mass M_A with an angle θ (in the c.o.m. frame). The c.o.m. recoil momentum, or momentum transfer, is

$$|\vec{q}|^2 = 2\mu_{\chi A}^2 v^2 (1 - \cos \theta), \quad \mu_{\chi A} = m_\chi M_A / (m_\chi + M_A). \quad (146)$$

The recoil energy imprinted on the nucleus is then

$$E_R = \frac{|\vec{q}|^2}{2M_A}. \quad (147)$$

which is maximum for $\theta = \pi$ ($|\vec{q}_{\max}| = 2\mu v$), so

$$E_R^{\max} = 2v^2 \frac{m_\chi^2 M_A}{(m_\chi + M_A)^2} = 2 \frac{\mu_{\chi A}^2 v^2}{M_A}. \quad (148)$$

Such a recoil energy of the scattered nucleus can be measured and can signal the occurrence of a DM particle scattering by.

As an examples to get an idea of the orders of magnitude involved: for a DM particle with mass $m_\chi = 100$ GeV scattering off a ^{131}Xe nucleus, we get

$$E_R^{\max} = 2 \left(\frac{v}{200 \text{ km/s}} \right)^2 \left(\frac{2}{3} 10^{-3} \right)^2 \frac{100^2 \cdot 131}{231^2} 10^6 \text{ keV} \simeq 22 \text{ keV} \left(\frac{v}{200 \text{ km/s}} \right)^2 \quad (149)$$

so the recoil energies are typically in the $\mathcal{O}(1 \div 10)$ keV range. The experiments are able to tag the event and measure E_R by directly observing one or two of the following 3 end-products: 1) heat; 2) ionization; 3) scintillation.

Let us make a back-of-the-envelope estimate of the expected number of events per unit of time. Consider a detector consisting of N_T nuclei with mass number A and mass $M_A \simeq A \cdot m_p \simeq A$ GeV. The total target mass of the detector is $M_T = N_T M_A$ (alternatively, the number density of target nuclei is $N_T = N_{\text{Avogadro}}/A$). Let $\sigma_{\chi A}$ be the nucleus-DM cross section, so

$$\begin{aligned} \frac{\# \text{ events}}{\text{time}} &= (\# \text{ targets}) \times (\text{WIMP flux on Earth}) \times (\text{cross section}) = N_T \left(\frac{\rho_\oplus}{M_\chi} v \right) \sigma_{\chi A} \\ &\simeq \frac{1 \text{ event}}{\text{yr}} \times \frac{M_T/A}{\text{kg}} \times \frac{\sigma}{10^{-39} \text{ cm}^2} \times \frac{\rho_\oplus}{0.3 \text{ GeV cm}^{-3}} \times \frac{v}{200 \text{ km/s}} \times \frac{100 \text{ GeV}}{m_\chi}. \end{aligned}$$

More precisely, the spectrum of events per recoil energies is given by

$$\frac{dR}{dE_R} = N_T \int_{|\vec{v}| > v_{\min}} |\vec{v}| \frac{d\sigma_{\chi A}}{dE_R} dn_{\text{DM}} = N_T \frac{\rho_\oplus}{m_\chi} \int_{|\vec{v}| > v_{\min}} d^3v |\vec{v}| f(\vec{v}, t) \frac{d\sigma_{\chi A}}{dE_R} \quad (150)$$

where we inserted the differential particle density

$$dn_{\text{DM}} = \frac{\rho_\oplus}{m_\chi} f(v) d^3v \quad (151)$$

with $f(v)$ being the velocity distribution and $v_{\min} = \sqrt{M_A E_R^{\text{th}} / (2\mu_{\chi A}^2)}$ is the minimal DM velocity needed to transfer a threshold kinetic energy E_R^{th} to the nucleus.

The most recent results for SI cross sections are from Xenon1T experiment [8] (about 2 tons of liquid Xe) are shown in Fig. 7. The SD cross section is much less constrained, a few orders of magnitude weaker bound than SI.

The characteristic shapes of the bounds can be understood as follows. The total event rate turns out to be proportional to $R \propto \sigma \mu_{\chi A}^2 / m_\chi < R_{\text{observed}}$. Therefore a bound on the total number of observed events translates into a limit on the coupling

$$\sigma < \sigma_{\text{bound}} \propto \frac{m_\chi}{\mu_{\chi A}^2} \sim \begin{cases} m_\chi^{-1} & (m_\chi \ll m_A) \\ m_\chi & (m_\chi \gg m_A) \end{cases} \quad (152)$$

This dependence explains the typical exclusion curves shown by the experimental collaborations, and have a dip (maximal exclusion) around $m_\chi \simeq m_A$ where the reduced mass is maximal.

The vector interactions mediated by Z exchange would typically lead to a spin-independent cross section $\sigma \sim \alpha_W^2 m_p^2 / M_Z^4 \approx 10^{-39} \text{ cm}^2$, which is already excluded by orders of magnitude.

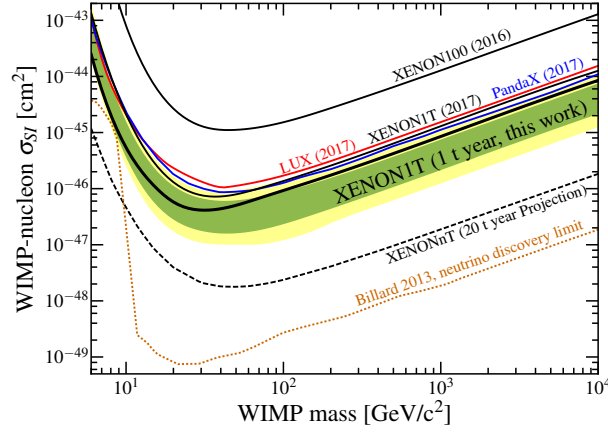


Fig. 7: 90% confidence level upper limit on spin-independent WIMP-nucleon cross section from XenonIT. A comparison with previous Xenon results, LUX and PandaX experiments is also shown. Figure from Ref. [8]

5.6 Indirect Detection

The indirect searches for DM are based on identifying excesses in fluxes of gamma rays/cosmic rays with respect to their presumed astrophysical backgrounds. These stable Standard Model particles may be the end product of the annihilation (or decay) of DM in the galactic halo or in the Sun. The schematic chain of processes leading from DM self-annihilations to observable fluxes at Earth is

$$\chi\chi \rightarrow \text{SM} \xrightarrow{\text{hadron./decay}} \text{SM} \xrightarrow{\text{stable species}} \xrightarrow{\text{astrophys. prop.}} \text{fluxes at Earth}. \quad (153)$$

Promising sources of DM annihilations are generically the regions where DM is expected to be the densest, such as the galactic center, the inner halo of our Galaxy, nearby galaxies dominated by DM, the center of the Sun, the center of the Earth. However, in some of these regions it is usually very complicated to understand the underlying astrophysics. So the best detection opportunities might come from selecting targets which are not necessarily the richest in DM but with well-identified backgrounds (favourable signal/background ratio). This also depends on which species of cosmic ray one is looking for.

The first step of the chain (153) DM annihilations into primary channels (like $q\bar{q}$, $\ell^+\ell^-$, W^+W^- , etc.) is controlled by the DM model lagrangian describing the elementary interactions of the DM particle with the SM. Once the primary products of annihilations are produced, they will undergo standard SM evolution, like decay, radiation, hadronization, controlled by QED, EW and QCD interactions. The end-product of this step is to have stable particle species (e.g. e^\pm , γ , ν , p etc.). Such stable particles are then travelling through the galaxy from their production point to the Earth, and they are subject to a number of astrophysical processes. Finally, the result of the astrophysical propagation of stable particles is the fluxes at detection (Earth) which is what can be measured.

This chain has to be reversed in order to extract information on the original DM model from observations of the fluxes. As it is clear, in this inversion process a lot of uncertainties come into play, especially those from the astrophysical propagation mechanisms.

The SM particles giving best information are photons, neutrinos and stable anti-particles: e.g. positrons and anti-protons (also, maybe, anti-deuteron, anti-helium). Why anti-matter? Because there is little anti-matter from early universe and (possibly) little anti-matter in primary cosmic rays. Observations provide a positron fraction of the order $e^+/(e^+ + e^-) \sim 0.1$ and an antiproton-to-proton ratio of the order $\bar{p}/p \sim 10^{-4}$. Each stable species has advantages and disadvantages to be used as a DM indirect detection probe:

- **Photons.** They freely propagate, in the galactic environment. However DM is electrically neutral,

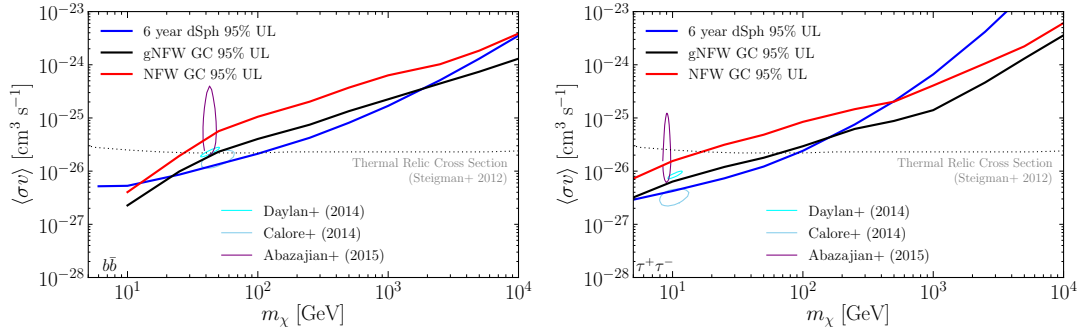


Fig. 8: DM upper limits on DM self-annihilation cross section from Fermi-LAT observations of the Galactic Center, as a function of the DM mass, for annihilations into $b\bar{b}$ (left panel) and $\tau^+\tau^-$ (right panel). The results are shown at the 95% confidence level assuming the generalized NFW (black) and NFW (red) DM profiles. The upper limits from the recent analysis of 15 dwarf spheroidal galaxies using 6 years of Fermi-LAT data are shown in blue. The dotted line indicates the thermal relic cross section. Figures taken from Ref. [9].

so that photons can be produced only via some subdominant mechanism (e.g. loops) or as secondary radiation (synchrotron, bremsstrahlung). The spectrum is suppressed, and the astrophysical background difficult.

- **Positrons.** They diffuse in the galactic magnetic fields with energy losses due to: synchrotron emission, Coulomb scattering, ionization, bremsstrahlung and inverse Compton. The DM contribution is dominated by the nearby regions of the galaxy. Below a few GeV, the effect of solar activity is important.
- **Anti-protons.** They diffuse in the galactic magnetic fields with negligible energy losses, until they scatter on matter. Therefore even far-away regions of the Galaxy can contribute to the flux collected on Earth and, as a consequence, its normalization has significant astrophysical uncertainties. Below a few GeV, the effect of solar activity is important.
- **Neutrinos.** TeV-scale neutrinos propagate freely in the Galaxy and can also propagate through the dense matter of the Sun and the Earth. Neutrinos are difficult to detect, they are measured indirectly via the detection of charged particles (e.g. muons) produced by a neutrino interaction in the rock or water surrounding a neutrino telescope. The incoming neutrino energy can only be partially reconstructed.

As an example, in Fig. 8 we show the upper limits on the self-annihilation cross section of DM from gamma-ray observations, in two different annihilation channels: $b\bar{b}$ and $\tau^+\tau^-$. The thermal relic cross section sets the reference to exclude models giving lower cross section (that would lead to too much DM abundance today), so one can exclude (e.g. using 6-year data on dwarf spheroidal galaxies) DM annihilating into $b\bar{b}$ or $\tau^+\tau^-$ with masses $m_\chi \lesssim 100$ GeV.

5.7 Collider Searches

How does DM (a WIMP) show up in a collider, such as the LHC? A WIMP must be stable (over collider scales) and very weakly interacting. So, even if a WIMP is produced in a high-energy collision, it escapes the detectors with no interaction, thus leaving no visible tracks. The DM behaves exactly like a neutrino, for collider purposes, so its unavoidable signal is just “missing energy”. This implies that the irreducible background of the DM searches (and very often the dominant background) is due to $Z \rightarrow \nu\bar{\nu}$ (e.g. with Z produced via Drell-Yan process).

If the DM is stabilized by an exact Z_2 symmetry under which it is odd, while the SM is even, then DM must be produced in pairs.

Since the missing energy alone is a rather poor signal, one needs something else as a handle to select events involving DM production. The identification of the most suitable extra handle, is a model-dependent issue. It may be jets or other objects from initial state radiation, accompanying particles, displaced vertices, etc.

At this point, an important *caveat* is in order: the LHC cannot discover the DM. It may only discover a weakly interacting particle with lifetime larger than the size of the detector, but there is not way to test the stability of the escaping particles on cosmological scales.

So far, there has been no signal for DM at LHC. There may be three reasons for that:

1. DM may not interact with ordinary matter: indeed, we are only sure that DM has gravitational interactions;
2. DM physics may not be accessible by LHC: e.g. DM may be too light/heavy or interacting too weakly with ordinary matter;
3. we may not have explored all the possibilities: DM may be buried under large backgrounds or hiding behind unusual/unexplored signatures.

The simplest handle to correlate with missing transverse energy (MET) is to consider the Initial State Radiation (ISR) of some SM particle X , where X may be a quark/gluon (producing a jet in the final state), a photon, a W/Z , or even a Higgs. This class of signatures are called mono- X searches. However, the mono-jet is what provides the strongest limits in most situations.

Mono- X +MET searches have the virtue of being rather general, the backgrounds are relatively well-known and they provide complementary/competitive results with direct detection. The main drawbacks are that some background is irreducible, there is a small signal-to-background ratio and the searches are limited by systematics.

Whether or not one chooses to explore DM at LHC using the mono- X signal, one very important question to ask is: which DM model to test? The interaction between quarks and DM can be modelled in many different ways. One can nonetheless divide the infinite-dimensional space of DM and Beyond-the-Standard-Model (BSM) theories into three broad categories:

1. Complete models. These are models of BSM physics like Supersymmetry, Composite Higgs, etc. which provide a valid description of elementary particles up to very high energies (ultraviolet complete), typically including also a solution of the hierarchy problem.
Pros: they are ultraviolet (UV) complete, motivated by BSM issues (like the hierarchy problem).
Cons: they have many parameters, and typically include sources of fine tuning.
2. Effective operators. They are coming from integrating out whatever heavy physics is responsible for mediating the SM-DM interactions, e.g. the heavy mediator. This approach has been often considered as “model-independent”, but it is not, since one needs to specify up the energy cutoff up to which the Effective Field Theory (EFT) is valid. This depends on the UV completion.
Pros: it is an economical approach (no need to specify mediators) and provide a common language to compare results from different experiments, e.g. direct/indirect detection. Cons: they are less complete than complete models; EFT is not always applicable, especially at very high energies involved in LHC processes.
3. Simplified models. They are a sort of mid-way between the two extremes described above. A heavy mediator particle, mediating the interactions between SM and DM, is exchanged in the s - or t -channel (for a review, see e.g. Ref [10]).
If the DM sector is more complicated than just an extra particle coupled to the SM, the heavy mediator approach is however a simple and good enough representation of what is going on. Simplified models are therefore simple versions of more complicated theories but with only the minimum amount of degrees of freedom which are necessary to model the physical process of interest.

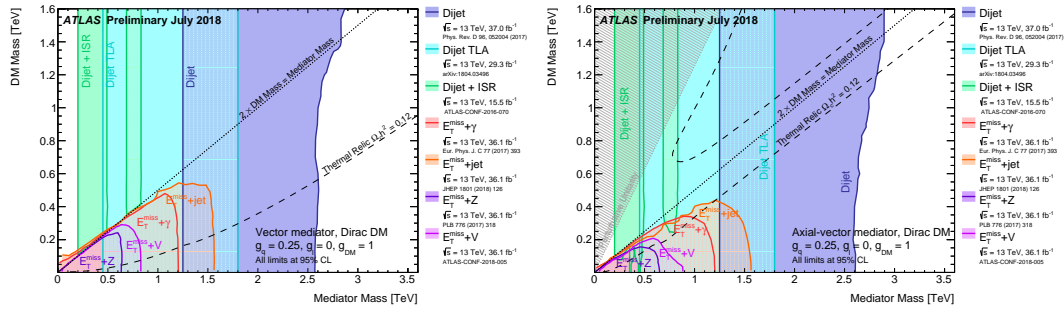


Fig. 9: Regions in a DM mass-mediator mass plane excluded at 95% CL by a selection of ATLAS dark matter searches, for vector mediator (left panel) and an axial-vector mediator (right panel) mediating the interactions between the SM and DM. Figures taken from ATLAS summary plots.

Pros: they provide a good representation of more complicated situations with minimum number of degrees of freedom; they are theoretically consistent. Cons: they require extra propagating degrees of freedom, beyond just the DM particle, so more parameters than EFTs; with a single simplified model it is hard to catch all phenomenological possibilities of complete models.

The great advantage of simplified models is that one can combine the search for the DM with the search for the mediator itself, e.g. looking for it as a di-jet resonance (see Fig. 9). As it is clear from Fig. 9, the di-jet searches for the mediators are actually setting stronger limits than the mono- $X + \text{MET}$ searches.

The limits in the DM mass-mediator mass plane can be recast into constraints on WIMP-nucleon scattering cross sections, to be compared with those from direct detection experiments. The main result is that for spin-independent couplings, the direct detection experiments set the most stringent limits (for $m_\chi \gtrsim 5$ GeV), but for spin-dependent couplings (for which direct detection is weaker) the LHC bounds are actually stronger.

Is this the whole story? The negative results of DM searches are calling for new efforts towards developing other tools and methodologies to increase the power of the searches. A couple of topics along this direction which are worth mentioning are: exploring less conventional, unexplored phenomenological signatures for DM; use data-driven approaches (e.g. machine learning) to get new and deeper views into the available and upcoming data.

6 Inflation

Inflation [11–13] is one of the basic ideas of modern cosmology and has become a paradigm for the physics of the early universe. In addition to solving the shortcomings of the standard Big Bang theory, inflation has received a great deal of experimental support, for example it provided successful predictions for observables like the mass density of the universe and the fluctuations of the cosmic microwave background radiation. Before discussing inflation in more detail, let us first review some background material about standard cosmology, which serves also to introduce the notation, and outline its major shortcomings.

6.1 Shortcomings of Big Bang Cosmology

Flatness problem. Recall from Eq. (45) that curvature parameter Ω_k is of the order of 0.1% (10^{-3}) today, which means that to a very good approximation we live in a flat universe. Let us define the total Omega parameter as

$$\Omega \equiv \frac{\rho_{\text{tot}}}{\rho_c} = \Omega_m + \Omega_r + \Omega_\Lambda. \quad (154)$$

From the sum rule of Omega parameters in Eq. (35) we get that

$$\Omega - 1 = \frac{k}{a^2 H^2}. \quad (155)$$

The parameter $|\Omega - 1|$ grows with time during radiation- and matter-dominated eras. In particular, during radiation domination $H^2 \propto \rho_{\text{radiation}} \propto a^{-4}$, so

$$|\Omega - 1| \propto \frac{1}{a^2 H^2} \propto \frac{1}{a^2 a^{-4}} \propto a^2. \quad (156)$$

Let us extrapolate this value back in time until the Planck time $t_P \sim 10^{-43}$ s

$$\frac{|\Omega - 1|_{T=T_P}}{|\Omega - 1|_{T=T_0}} \approx \left(\frac{a(t_P)}{a(t_0)} \right)^2 \approx \left(\frac{T_0}{T_P} \right)^2 \approx 10^{-64}. \quad (157)$$

Since we observe today that the energy density of the universe is very close to the critical density (i.e. a very small Ω_k) the Ω parameter must have been close to unity to an extremely high accuracy (of about one part in 10^{64} if we start the radiation-dominated era at the Planck time. Therefore, an extreme degree of fine tuning is necessary to arrange such a precise initial value of the density parameter of the universe. This is the flatness (or fine-tuning) problem.

Entropy problem. The flatness problem is also connected to the entropy problem, which is understanding why the total entropy of the visible universe is incredibly large. In fact, recall that the entropy in a comoving volume of radius a and temperature T is $S \simeq (aT)^3$ = which is constant, and today the entropy within the horizon is

$$S_0 \sim H_0^{-3} s_0 \sim H_0^{-3} T_0^3 \sim 10^{90}, \quad (158)$$

which is huge with respect to that in the early universe. During radiation domination the Hubble parameter is $H \sim T^2/M_P$, where the Planck mass is $M_P \equiv G^{-1/2} = 1.22 \times 10^{19}$ GeV, so Eq. (155) can be re-written as

$$|\Omega - 1| \propto 1 a^2 H^2 \propto \frac{1}{a^2 T^4} \propto \frac{1}{T^2 S^{2/3}}. \quad (159)$$

This relation tells us that Ω at early times is so close to 1 because the total entropy of the universe is enormous. For example, at the Planck scale, the entropy of 10^{90} corresponds to $\Omega - 1 \sim 10^{-60}$.

Horizon problem. As already mentioned in Section 4.3, the CMB has an amazingly high degree of homogeneity, about one part in 10^5 . But this poses a serious problem for cosmology. Recall from Section 2.2.8 that the particle horizon is the distance travelled by photons. Let us consider our current particle horizon d_0 and track it back in time to the time of photon decoupling (last scattering), when CMB formed $T_{\text{dec}} \sim 0.3$ eV. The CMB temperature today is $T_0 \simeq 2.3 \times 10^{-4}$ eV, so particle horizon at dec

$$\lambda_H|_{\text{dec}} = d_0 \frac{a_{\text{dec}}}{a_0} = d_0 \frac{T_0}{T_{\text{dec}}}. \quad (160)$$

From the Friedmann equation we know that during matter domination (from photon decoupling to today) the Hubble radius, i.e. the size of the observable universe, redshifts as $a^{-3/2} \sim T^{3/2}$. Therefore

$$\left(\frac{\lambda_H|_{\text{dec}}}{H_{\text{dec}}^{-1}} \right)^3 = \left(\frac{T_{\text{dec}}}{T_0} \right)^{3/2} \approx 10^5. \quad (161)$$

So this result is telling us that when CMB formed, the length λ_H corresponding to our universe today was much larger (by a factor 10^5) than the size of the causally connected universe at that time (H_{dec}^{-1}). So at photon decoupling there were 10^5 causally disconnected regions that now correspond to our horizon! In other words, the photons received today were emitted from regions that were causally disconnected

at the time of photon decoupling, because they were out of the particle horizon. Why regions that were not in causal contact share the same temperature to a very high precision? This is the so-called horizon problem.

Monopole problem. Lastly, another issue that was plaguing the Standard Big Bang Cosmology in the context of Grand Unified Theories (GUTs) is the overproduction of magnetic monopoles. Indeed, magnetic monopoles are a generic prediction of GUTs and they are produced at a phase transition at $T = T_c$, after which they behave as non-relativistic matter. To estimate the number density of monopoles, we consider the simple argument of expecting approximately 1 monopole per correlation volume ℓ_{cor}^3 , where the correlation length is bounded by the horizon at the critical temperature $\ell_{\text{cor}} \lesssim H(T_c)^{-1}$. Therefore, the number density of monopoles is roughly given by

$$n_M \simeq \ell_{\text{cor}}^{-3} \gtrsim H(T_c)^3 \simeq \left(1.66\sqrt{g_*(T_c)}\right)^3 \frac{T_c^6}{M_P^3} \implies \frac{n_M}{s} \sim \sqrt{g_*(T_c)} \left(\frac{T_c}{M_P}\right)^3 \quad (162)$$

their number density behaves like $n_M(t) \propto a^{-3}(t) \propto s(t)$, and therefore using (162) we can estimate the abundance of magnetic monopoles today as

$$\begin{aligned} \rho_M(T_0) &= m_M n_M(T_0) = m_M \frac{n_M(T_c)}{s(T_c)} s(T_0) \sim m_M \sqrt{g_*(T_c)} \left(\frac{T_c}{M_P}\right)^3 g_*(T_0) T_0^3 \\ &\sim 10^{12} \left(\frac{m_M}{10^{16} \text{ GeV}}\right) \left(\frac{T_c}{10^{16} \text{ GeV}}\right)^3 \sqrt{\frac{g_*(T_c)}{10^2}} \text{ GeV cm}^{-3} \end{aligned} \quad (163)$$

while the critical density is $\rho_c \simeq 10^{-5} \text{ GeV cm}^{-3}$, so

$$\frac{\rho_M}{\rho_c} \sim 10^{17}, \quad (164)$$

for monopoles with GUT-scale mass ($\sim 10^{16} \text{ GeV}$). This overabundance of magnetic monopoles is the so-called monopole problem. Therefore, one should suppose either that the universe was never at temperatures as high as $T_c \sim 10^{16} \text{ GeV}$, or that Grand Unification is not there. The monopole problem was the primary motivation behind the idea of inflation.

6.2 The inflationary solution

Inflation elegantly solves at once the problems associated with the standard Big Bang cosmology. The inflationary era is defined as the epoch in the early history of the universe when it underwent a period of accelerated expansion

$$\ddot{a} > 0. \quad (165)$$

According to Eq. (25), this condition is equivalent to $\rho + 3p < 0$ (for negligible cosmological constant). For the sake of simplicity, we shall only consider here a more stringent condition for inflation, $p = -\rho$ (negative pressure!). This condition is also known as de Sitter phase, and corresponds to constant energy density and Hubble parameter H_I , and thus the scale factor grows exponentially in time

$$a(t) \propto e^{H_I t}. \quad (166)$$

Inflation delivers a flat universe, thus providing an explanation for the initial condition that Ω is close to 1 to a high precision. In fact, during inflation, the Hubble rate is nearly constant and the curvature parameter $\Omega - 1$ is proportional to $1/a^2$ (see Eq. (155)), thus its final value at the end of inflation $t = t_f$ is related to the primordial initial value at $t = t_i$ by

$$\frac{|\Omega - 1|_{\text{final}}}{|\Omega - 1|_{\text{initial}}} = \left(\frac{a(t_i)}{a(t_f)}\right)^2 = e^{-H_I(t_f - t_i)}. \quad (167)$$

If inflation lasts for long enough, the Ω parameter will be exponentially driven to unity. Therefore, the universe emerging at the end of inflation is spatially flat to a very high accuracy.

Furthermore, the large amount of entropy produced during the non-adiabatic phase transition from the end of inflation and the beginning of the radiation-dominated era also produces a huge entropy

$$\frac{S_f}{S_i} \sim \left(\frac{a(t_f)}{a(t_i)} \right)^3 \left(\frac{T_f}{T_i} \right)^3 \sim e^{3H_I(t_f-t_i)} \left(\frac{T_f}{T_i} \right)^3. \quad (168)$$

Therefore, a period of exponential expansion can easily account for a large amount of entropy and it can greatly dilute all magnetic monopoles down to an unobservable level.

If the universe underwent a period when the physical scales evolve faster than the horizon scale, it is possible to make the CMB photons in causal contact at some primordial time before the photon decoupling. The physical size of a perturbation grows as the scale factor: $\lambda \sim a$, while the horizon scale is $H^{-1} = a/\dot{a}$. If a period exists in the early history of the universe when

$$\frac{d}{dt} \frac{\lambda}{H^{-1}} = \ddot{a} > 0, \quad (169)$$

the CMB photons may have been in causal contact at that time, thus explaining the high level of homogeneity and isotropy observed in the CMB today. Such an epoch of accelerated expansion is precisely the inflationary stage.

The mechanism of inflation can be simply realized by means of a scalar field ϕ , called the inflaton, whose energy is dominant in the universe and with potential energy $V(\phi)$ much larger than the kinetic energy. The generic lagrangian for the inflaton is

$$\mathcal{L} = \frac{1}{2} \partial_\mu \phi \partial^\mu \phi - V(\phi), \quad (170)$$

while the energy-momentum tensor is

$$T^{\mu\nu} = \partial^\mu \phi \partial^\nu \phi - g^{\mu\nu} \mathcal{L}. \quad (171)$$

Neglecting the spatial gradients, the 00 and ii components of the energy-momentum tensor, corresponding to the energy density and the pressure of the inflaton respectively, are given by

$$T^{00} = \rho_\phi = \frac{\dot{\phi}^2}{2} + V(\phi), \quad (172)$$

$$T^{ii} = p_\phi = \frac{\dot{\phi}^2}{2} - V(\phi). \quad (173)$$

If the kinetic energy is negligible with respect to the potential energy

$$V(\phi) \gg \dot{\phi}^2, \quad (174)$$

and if the energy density of the inflaton dominates over other forms of energy density (such as matter or radiation), then we would have a de Sitter stage $p_\phi = -\rho_\phi$ and the Friedmann equation would read

$$H^2 \simeq \frac{8\pi G_N}{3} V(\phi). \quad (175)$$

Thus, inflation is driven by the vacuum energy of the inflaton field.

The equation of motion of the inflaton field in an expanding universe is

$$\ddot{\phi} + 3H\dot{\phi} + V'(\phi) = 0, \quad (176)$$

where the prime refers to the derivative with respect to ϕ . When $V(\phi) \gg \dot{\phi}^2$ and $\ddot{\phi} \ll 3H\dot{\phi}$, the scalar field “slowly rolls” down its potential. Under the slow-roll conditions, the equation of motion reduces to

$$3H\dot{\phi} \simeq -V'(\phi). \quad (177)$$

It is straightforward to derive some important relations from the two equations in Eqs. (175) and (177) and the slow-roll condition in Eq. (174). From Eqs. (175) and (177) one can show that

$$\dot{H} = -4\pi G_N \dot{\phi}^2, \quad (178)$$

while using Eqs. (174) and (177) one obtains

$$\frac{(V')^2}{V} \ll H^2, \quad (179)$$

and finally using Eqs. (174), (175), (177) and (178) we arrive at

$$V'' \ll H^2. \quad (180)$$

It is customary to define the “slow-roll parameters” ϵ, η as

$$\epsilon \equiv \frac{1}{16\pi G_N} \left(\frac{V'}{V} \right)^2, \quad (181)$$

$$\eta \equiv \frac{1}{8\pi G_N} \left(\frac{V''}{V} \right). \quad (182)$$

in such a way that the conditions Eqs. (179)-(180) derived by the slow-roll regime can be simply recast into $\epsilon \ll 1, |\eta| \ll 1$. Furthermore, from the Friedmann equation (175) and Eq. (178), one can rewrite the ϵ parameter as

$$\epsilon = -\frac{\dot{H}}{H^2} \quad (183)$$

which allows one to express the second derivative of the scale factor in terms of ϵ

$$\frac{\ddot{a}}{a} = \dot{H} + H^2 = (1 - \epsilon)H^2 > 0 \iff \epsilon < 1. \quad (184)$$

So the condition defining inflation $\ddot{a} > 0$ is equivalent to $\epsilon < 1$, and inflation ends when $\epsilon \simeq 1$.

6.3 Consequences of inflation

Spectral Parameters. As the inflaton rolls down its potential energy, it undergoes two kind of fluctuations: a classical one and a quantum one. During a Hubble time H^{-1} , these fluctuations behave as

$$(\delta\phi)_{\text{cl}} \sim \dot{\phi} H^{-1}, \quad (185)$$

$$(\delta\phi)_{\text{qu}} \sim H/(2\pi). \quad (186)$$

The so-called power spectrum of scalar perturbations is given by the ratio of these two kinds of fluctuations at a momentum scale k equal to the horizon scale aH

$$\mathcal{P}(k) = \left[\frac{(\delta\phi)_{\text{qu}}}{(\delta\phi)_{\text{cl}}} \right]^2 = \left(\frac{H}{\dot{\phi}} \right)^2 \left(\frac{H}{2\pi} \right)^2 \Big|_{k=aH}, \quad (187)$$

and after some manipulations we arrive at the expression in terms of the slow-roll parameter ϵ

$$\mathcal{P}(k) = \frac{8G_N^2 V}{3 \epsilon} \Big|_{k=aH} \quad (188)$$

The spectral index n_s is defined as

$$n_s - 1 \equiv \frac{d \ln \mathcal{P}(k)}{d \ln k} \quad (189)$$

which can be interpreted as the exponent of the k -dependence of the power spectrum $\mathcal{P}(k) \propto k^{n_s-1}$. It is easy to show that

$$\frac{d}{d \ln k} = -\frac{1}{8\pi G_N} \frac{V'}{V} \frac{d}{d\phi} \quad (190)$$

from which it follows that

$$\frac{d\epsilon}{d \ln k} = -2\epsilon\eta + 4\epsilon^2 \quad (191)$$

and finally the spectral index in terms of the slow-roll parameters is

$$n_s = 1 - 6\epsilon + 4\eta. \quad (192)$$

So, in slow-roll inflation where $\epsilon, |\eta| \ll 1$, the spectral index is very close to 1, meaning that the spectrum of scalar perturbations is nearly scale-independent.

Other kinds of perturbations are the so-called tensor perturbations (or gravity waves), whose power spectrum turns out to be

$$\mathcal{P}_g = \frac{128\pi G_N^2}{3} V \Big|_{k=aH}, \quad (193)$$

from which one can derive the important tensor-to-scalar ratio r

$$r = \frac{\mathcal{P}_g}{\mathcal{P}} = 16\epsilon \ll 1, \quad (194)$$

which is also predicted as very small in slow-roll inflation.

Evolution of Perturbations. The Fourier expansion of inflaton field fluctuations in k -modes can be written as

$$\delta\phi(\mathbf{x}, t) = \int \frac{d^3k}{(2\pi)^3} e^{i\mathbf{k}\cdot\mathbf{x}} \delta\phi_k(t), \quad (195)$$

and the k -modes obey the equation of motion

$$\delta\ddot{\phi}_k + 3H\delta\dot{\phi}_k + \frac{k^2}{a^2}\delta\phi_k = 0. \quad (196)$$

This can be studied more easily in two extreme regimes, according to whether the modes are inside or outside the horizon. The modes inside the horizon are characterized by a length scale $\lambda \propto (a/k) \ll H^{-1}$, which is equivalent to the condition $k \gg aH$, so the equation of motion reads

$$\delta\ddot{\phi}_k + \frac{k^2}{a^2}\delta\phi_k = 0. \quad (197)$$

This is a simple harmonic oscillator with $\delta\phi_k \propto \lambda^{-1}$, so fluctuations are stretched during inflation.

The modes outside the horizon are characterized by a length scale $\lambda \propto (a/k) \gg H^{-1}$, which is equivalent to $k \ll aH$, so the equation of motion reads

$$\delta\ddot{\phi}_k + 3H\delta\dot{\phi}_k = 0. \quad (198)$$

This is an oscillator with friction, and the corresponding fluctuations are constant (“frozen”).

So the fluctuations of the inflaton field grow exponentially during inflation, until their wavelength exits the horizon; then fluctuations get frozen outside the horizon; after inflation ends, fluctuations re-enter the horizon (see Figure 10 for a pictorial representation).

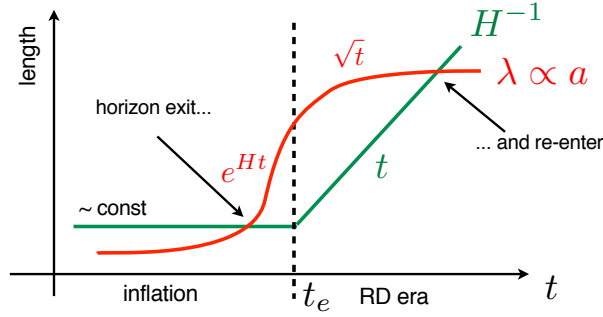


Fig. 10: Evolution of the length scales ($\lambda \propto a$) during and after inflation, in red. For comparison, in green it is shown the evolution of the Hubble scale H^{-1} , during inflation and after inflation (in the radiation-dominated epoch).

CMB and Large-scale structures. Inflation can also be responsible for the physical processes giving rise to the CMB anisotropies and the matter structures we observe in the universe today. In fact, primordial small quantum fluctuations of the energy density are excited during inflation and stretched to cosmological scales; then they exit the horizon and get frozen; when they re-enter the horizon at some matter- or radiation-dominated epoch, these fluctuations will start growing giving rise to the formation of all the structures we observe.

Physically, the mechanism works because the fluctuations are connected to the metric perturbations (gravity) via Einstein's equations and gravity acts as a messenger: once a given wavelength re-enters the horizon, gravity communicates the perturbations to baryons and photons. Therefore, the primordial quantum fluctuations of the inflaton field during inflation provide the seeds of the CMB temperature fluctuations and the large-scale structures observed today.

7 Baryogenesis

Our universe has a matter-antimatter asymmetry. We observe our universe to consist of matter, and not antimatter in appreciable quantities. More precisely, the difference between the number density of baryons and that of anti-baryons is expressed in terms of the baryon-to-photon ratio today

$$\eta \equiv \frac{n_B - n_{\bar{B}}}{n_\gamma} \Big|_0, \quad (199)$$

(recall that the photon number density is $n_\gamma = 2\zeta(3)T^3/\pi^2$). The accurate measurement of the matter-antimatter asymmetry has been mainly provided by two independent and solid types of experiments.

- Big Bang Nucleosynthesis. We have already discussed in Section 3 that the simultaneous fit to primordial element abundances in terms of the single free parameter η is a remarkable success of standard cosmology and provides

$$5.2 \times 10^{-10} < \eta < 6.6 \times 10^{-10} \quad (95\% \text{ CL}). \quad (200)$$

- Cosmic Microwave Background. The position and height of acoustic peaks in the power spectrum of CMB temperature anisotropies, probing the baryon/photon fluid at the last scattering surface, allow us to constrain the baryon energy density and therefore η [1]:

$$\eta = (6.13 \pm 0.04) \times 10^{-10}, \quad (201)$$

The agreement of these two independent measurements is evident. Within the standard cosmological model η is not predicted, it is a free parameter whose value is fixed by observations. Explaining this number is challenging, and a definitive answer is still missing.

If there was an era of cosmological inflation, any initial asymmetry would have been diluted by the enormous entropy increase during such epoch; hence, at the end of inflation the universe looks perfectly symmetric. Therefore, explaining the origin of the tiny (but non-zero) asymmetry we observe today requires that some post-inflationary mechanism is at work. The mechanism by which a baryon asymmetry is dynamically produced in the early universe is generically called baryogenesis.

In 1967 Sakharov pointed out three necessary conditions for a baryon asymmetry to be produced in the early universe and observed today:

I. Baryon number violation.

This condition is quite obvious. Let us suppose to start from a baryon symmetric universe $B(t_0) = 0$, at a certain t_0 . The quantum mechanical evolution of the operator B is $B(t) \propto \int_{t_0}^t [B, H] dt'$, where H is the hamiltonian of the system. If B is conserved, $[B, H] = 0$ and then $B(t) = 0$ at all times.

II. C and CP violation.

If C were an exact symmetry, the probability of the process $i \rightarrow f$ would be equal to the one of the conjugated process $\bar{i} \rightarrow \bar{f}$. Therefore the same amount of f and \bar{f} would be present in the final state. But B is odd under C , so $B(\bar{f}) = -B(f)$ and so the net baryon number B would vanish.

Due to the CPT theorem, CP invariance is equivalent to T invariance and this implies that the probability of the process $i(\mathbf{r}_i, \mathbf{p}_i, \mathbf{s}_i) \rightarrow f(\mathbf{r}_j, \mathbf{p}_j, \mathbf{s}_j)$ is equal to that of the time-reversed process $f(\mathbf{r}_j, -\mathbf{p}_j, -\mathbf{s}_j) \rightarrow i(\mathbf{r}_i, -\mathbf{p}_i, -\mathbf{s}_i)$, where $\mathbf{r}_i, \mathbf{p}_i, \mathbf{s}_i$ denote coordinate, momentum and spin of the i -th particle, respectively. After performing an integration over all momenta and summation over all spins, the total baryon asymmetry vanishes.

III. Departure from thermal equilibrium.

Let us consider a species ψ carrying baryon number and being in thermal equilibrium, and distinguish the situations when it does or does not have a chemical potential.

If ψ has zero chemical potential, the CPT invariance implies that particles and anti-particles have the same mass and therefore $n_\psi = n_{\bar{\psi}}$, which implies $B \propto n_\psi - n_{\bar{\psi}} = 0$.

If ψ has chemical potential μ_ψ and is in chemical and thermal equilibrium and takes part in the B -violating process $\psi\psi \rightarrow \bar{\psi}\bar{\psi}$ (first Sakharov condition), then the relation $\mu_\psi = \mu_{\bar{\psi}}$ must hold. But on the other hand it must be that $\mu_{\bar{\psi}} = -\mu_\psi$, implying that μ_ψ must vanish and the previous argument applies.

Are these conditions met in the Standard Model (SM)? No.

1. In the SM the baryon number symmetry is anomalous so B -violation is present at a quantum level. The baryon (B) and lepton (L) numbers are exactly conserved at a classical level. But at a quantum level, these symmetries fail to be exact, they are anomalous.
2. The only source of CP -violation within the SM is provided by the complex phase of the CKM matrix. But it is too small to explain the observed baryon asymmetry because it is suppressed by small quark masses.
3. The departure from thermal equilibrium could be attained during the electroweak phase transition. Unfortunately, for the phase transition being strong enough to assure departure from equilibrium the Higgs mass should be $m_h \lesssim 60$ GeV, excluded by experimental data.

Therefore the baryon asymmetry is somehow linked to new physics beyond the SM, which is why it is so interesting. Any successful model of baryogenesis needs some new ingredient to be added to the SM. Because of our ignorance about what there is at energy scales well above TeV, one has to postulate some physics at those scales, check that the three Sakharov conditions are fulfilled and compute the generated baryon asymmetry.

Many models of baryogenesis have been proposed so far. Some of the most interesting and most popular ones are

– **Out-of-equilibrium decay.**

The out-of-equilibrium decay of a heavy boson provides a viable mechanism for successful baryogenesis. Such a heavy boson may be embedded in a Grand Unified Theory (GUT). Let us suppose that a heavy scalar particle X of mass M_X couples to the SM fermions f and has B -violating decay modes.

At high temperatures $T \gg M_X$, all particles are in thermal equilibrium and follow their equilibrium number densities. The reactions $X(\bar{X}) \leftrightarrow f\bar{f}$ are in equilibrium. The number density of X, \bar{X} track the equilibrium number density, $n_{X,\bar{X}} = n_X^{\text{eq}}$, so $B = 0$.

When the temperature lowers to $T \lesssim M_X$, the lifetime of X is of the order of the age of the universe $\Gamma_X^{-1} \sim H^{-1}$, and the interactions maintaining the number densities of X, \bar{X} at their equilibrium value are not so effective anymore, provided that the X is sufficiently heavy. So the decays and inverse decays of $X(\bar{X}) \leftrightarrow f\bar{f}$ slow down and the X particles become overabundant with respect to their equilibrium distribution; this is the departure from thermal equilibrium needed for baryogenesis.

If the X decay violates baryon number B , a net baryon number is produced for each decay, which would be erased by the opposite baryon asymmetry generated by the decay of \bar{X} . So we need the condition that C, CP are violated in the decays, i.e. $\text{BR}(X \rightarrow f\bar{f}) \neq \text{BR}(\bar{X} \rightarrow f\bar{f})$. These conditions ensure that a net baryon asymmetry is produced for each decay of X, \bar{X} .

– **Baryogenesis via Leptogenesis.**

A lepton asymmetry is produced in the early universe by out-of-equilibrium decay of heavy right-handed neutrinos. Such asymmetry is then reprocessed at the electroweak scale into a baryon asymmetry (by sphalerons). The mechanism of producing a net lepton asymmetry is similar to the one described for the out-of-equilibrium decay scenario. The appeal of leptogenesis is that it is built in see-saw models motivated by explaining the light neutrino masses.

– **Electroweak Baryogenesis.**

It is a rather complex mechanism aiming at realizing baryogenesis at the electroweak phase transition, by adding new physics at the electroweak scale that would allow the phase transition to be “strong” enough to provide enough baryon asymmetry. The SM needs to be extended by new extra bosonic degrees of freedom. The generic prediction is the presence of new CP-violating phases in the theory, which may be probed by experiments looking for electron and neutron electric dipole moments.

In conclusion, the cosmology/particle physics interplay has been and currently is a very successful and fascinating *liaison*, which may hold for us even more exciting surprises in the near future.

Acknowledgements

We wish to thank the organizers of the School for their kind invitation to give these lectures and their excellent work in running the School so successfully, and all the students for their active participation and insightful questions.

References

- [1] N. Aghanim *et al.* [Planck Collaboration], “Planck 2018 results. VI. Cosmological parameters,” arXiv:1807.06209 [astro-ph.CO].
- [2] R. H. Cyburt, B. D. Fields, K. A. Olive and T. H. Yeh, “Big Bang Nucleosynthesis: 2015,” Rev. Mod. Phys. **88**, 015004 (2016) doi:10.1103/RevModPhys.88.015004 [arXiv:1505.01076 [astro-ph.CO]].
- [3] E. W. Kolb and M. S. Turner, The Early universe, Addison-Wesley (New York, 1990).
- [4] D. S. Gorbunov, V. A. Rubakov, “Introduction to the Theory of the Early universe - Hot Big Bang Theory”, World Scientific (2011).

- [5] V. Mukhanov, “Physical Foundations of Cosmology”, Cambridge University Press (2005).
- [6] D. Clowe, M. Bradac, A. H. Gonzalez, M. Markevitch, S. W. Randall, C. Jones and D. Zaritsky, “A direct empirical proof of the existence of dark matter,” *Astrophys. J.* **648**, L109 (2006) doi:10.1086/508162 [astro-ph/0608407].
- [7] K. G. Begeman, A. H. Broeils and R. H. Sanders, “Extended rotation curves of spiral galaxies: Dark haloes and modified dynamics,” *Mon. Not. Roy. Astron. Soc.* **249**, 523 (1991).
- [8] E. Aprile *et al.* [XENON Collaboration], “Dark Matter Search Results from a One Ton-Year Exposure of XENON1T,” *Phys. Rev. Lett.* **121**, no. 11, 111302 (2018) doi:10.1103/PhysRevLett.121.111302 [arXiv:1805.12562 [astro-ph.CO]].
- [9] M. Ackermann *et al.* [Fermi-LAT Collaboration], “The Fermi Galactic Center GeV Excess and Implications for Dark Matter,” *Astrophys. J.* **840**, no. 1, 43 (2017) doi:10.3847/1538-4357/aa6cab [arXiv:1704.03910 [astro-ph.HE]].
- [10] A. De Simone and T. Jacques, “Simplified models vs. effective field theory approaches in dark matter searches,” *Eur. Phys. J. C* **76**, no. 7, 367 (2016) doi:10.1140/epjc/s10052-016-4208-4 [arXiv:1603.08002 [hep-ph]].
- [11] A. H. Guth, “The Inflationary universe: A Possible Solution To The Horizon And Flatness Problems,” *Phys. Rev. D* **23** (1981) 347.
- [12] A. D. Linde, “A New Inflationary universe Scenario: A Possible Solution Of The Horizon, Flatness, Homogeneity, Isotropy And Primordial Monopole Problems,” *Phys. Lett. B* **108**, 389 (1982).
- [13] A. Albrecht and P. J. Steinhardt, “Cosmology For Grand Unified Theories With Radiatively Induced Symmetry Breaking,” *Phys. Rev. Lett.* **48**, 1220 (1982).